The EMBO Journal (2010) 29, 3571–3589 | © 2010 European Molecular Biology Organization | All Rights Reserved 0261-4189/10
www.embojournal.org

THE EMBO JOURNAL

Inhibition of mitochondrial fusion by α-synuclein is rescued by PINK1, Parkin and DJ-1

Frits Kamp[1,2,7,*], Nicole Exner[1,2,7], Anne Kathrin Lutz[3,7], Nora Wender[4], Jan Hegermann[4], Bettina Brunner[1,2], Brigitte Nuscher[1,2], Tim Bartels[2], Armin Giese[5], Klaus Beyer[2,6], Stefan Eimer[4], Konstanze F Winklhofer[3] and Christian Haass[1,2,*]

[1]DZNE-German Center for Neurodegenerative Diseases, Munich, Germany, [2]Adolf-Butenandt-Institute, Biochemistry, Ludwig-Maximilians-University, Munich, Germany, [3]Adolf-Butenandt-Institute, Neurobiochemistry, Ludwig-Maximilians-University, Munich, Germany, [4]European Neuroscience Institute Goettingen and DFG Research Center for Molecular Physiology of the Brain (CMPB), Goettingen, Germany, [5]Center for Neuropathology and Prion Research, Ludwig-Maximilians-University, Munich, Germany and [6]Department of Chemistry, The University of Arizona, Tucson, AZ, USA

Aggregation of α-synuclein (αS) is involved in the pathogenesis of Parkinson's disease (PD) and a variety of related neurodegenerative disorders. The physiological function of αS is largely unknown. We demonstrate with *in vitro* vesicle fusion experiments that αS has an inhibitory function on membrane fusion. Upon increased expression in cultured cells and in *Caenorhabditis elegans*, αS binds to mitochondria and leads to mitochondrial fragmentation. In *C. elegans* age-dependent fragmentation of mitochondria is enhanced and shifted to an earlier time point upon expression of exogenous αS. In contrast, siRNA-mediated downregulation of αS results in elongated mitochondria in cell culture. αS can act independently of mitochondrial fusion and fission proteins in shifting the dynamic morphologic equilibrium of mitochondria towards reduced fusion. Upon cellular fusion, αS prevents fusion of differently labelled mitochondrial populations. Thus, αS inhibits fusion due to its unique membrane interaction. Finally, mitochondrial fragmentation induced by expression of αS is rescued by coexpression of PINK1, parkin or DJ-1 but not the PD-associated mutations PINK1 G309D and parkin Δ1–79 or by DJ-1 C106A.

The EMBO Journal (2010) **29,** 3571–3589. doi:10.1038/emboj.2010.223; Published online 14 September 2010
Subject Categories: membranes & transport; neuroscience
Keywords: α-synuclein; mitochondria; neurodegeneration; Parkinson's disease

*Corresponding authors. F Kamp or C Haass, DZNE-German Center for Neurodegenerative Diseases, Adolf Butenandt-Institute, Biochemistry, Ludwig-Maximilians-University, Schillerstrasse 44, 80336, Munich, Germany. Tel.: +49 89 2180 75472; Fax: +49 89 2180 75415; E-mails: fkamp@med.uni-muenchen.de or chaass@med.uni-muenchen.de
[7]These authors contributed equally to this work

Received: 16 February 2010; accepted: 12 August 2010; published online: 14 September 2010

Introduction

A characteristic feature of Parkinson's disease (PD) is the intracellular deposition of Lewy bodies, which are predominantly composed of α-synuclein (αS). This 140 amino acid protein is widely distributed throughout the brain and expressed at high levels in neurons where it can reach concentrations of 0.5–1% of total protein (i.e. 30–60 μM) (Iwai *et al*, 1995; Spillantini *et al*, 1997; Bodner *et al*, 2009). In Lewy bodies, αS is arranged in fibrils with a β-sheet like structure (Der-Sarkissian *et al*, 2003; Chen *et al*, 2007). It is assumed that the pathogenicity of αS is associated with aggregation of the protein, which involves formation of small neurotoxic oligomers that eventually mature to larger insoluble deposits (Lee *et al*, 2004a; Haass and Selkoe, 2007; Kramer and Schulz-Schaeffer, 2007; Kostka *et al*, 2008; Kayed *et al*, 2009). A similar cascade of protein aggregation and precipitation is causative for the onset of other neurodegenerative diseases, such as Alzheimer's disease (Dobson, 2003; Haass and Selkoe, 2007).

A remarkable property of αS is its structural flexibility (Davidson *et al*, 1998; Beyer, 2007; Uversky, 2007). The protein is essentially unstructured in dilute aqueous solution (Uversky, 2002), whereas α-helical folding occurs upon binding to lipid surfaces. The NMR-derived structure of SDS-micelle-bound αS revealed two anti-parallel aligned amphipathic α-helices, the 'N-helix' spanning residues 3 through 37 and the 'C-helix' spanning residues 45 through 92. The C-terminal domain, which contains approximately 40 amino acids of which 14 are negatively charged and 2 positively charged, remains unstructured (Lee *et al*, 2004b; Ulmer and Bax, 2005; Ulmer *et al*, 2005). The structure of membrane-bound αS cannot be resolved by NMR as the rotation of vesicles is too slow. However, other biophysical techniques including electron spin resonance and circular dichroism (CD) revealed that α-helical folding also occurs for the N-terminal region when αS binds to membranes (Nuscher *et al*, 2004; Beyer, 2007; Jao *et al*, 2008; Drescher *et al*, 2008a). However, whether membrane-bound αS assumes a single extended α-helix, a broken helix or multiple structures (including oligomers) is unclear (Drescher *et al*, 2008a, b; Bodner *et al*, 2009; Ferreon *et al*, 2009; Perlmutter *et al*, 2009; Trexler and Rhoades, 2009). It has also been reported that αS binds to synaptic vesicles (Maroteaux *et al*, 1988; Jensen *et al*, 1998; Abeliovich *et al*, 2000; Kahle *et al*, 2000; Murphy *et al*, 2000; Cabin *et al*, 2002; Chandra *et al*, 2004, 2005; Jo *et al*, 2004; Yavich *et al*, 2004; Larsen *et al*, 2006; Ben Gedalya *et al*, 2009) as well as to mitochondria (Martin *et al*, 2006; Nakamura *et al*, 2008; Shavali *et al*, 2008). Biophysical studies from our laboratory revealed that binding of αS to highly curved bilayers leads to a stabilization of defects in the lipid packing (Nuscher *et al*, 2004; Cornell and Taneva, 2006; Kamp and Beyer, 2006). This motivated us to investigate whether αS could have an impact on membrane fusion.

So far little is known about the biological consequences of binding of αS to intracellular membranes. Studies in yeast

revealed that overexpression of αS leads to cellular toxicity by interfering with vesicular transport between the endoplasmic reticulum and the Golgi complex (Cooper *et al*, 2006). Fragmentation of the Golgi apparatus was also reported in neurons containing Pale bodies, pathological deposits known as early stages of Lewy bodies (Gosavi *et al*, 2002; Fujita *et al*, 2006; Lee *et al*, 2006). Moreover, functional impairment of mitochondria was caused by expression of wild type or mutant αS (Hsu *et al*, 2000; Orth *et al*, 2003; Smith *et al*, 2005; Parihar *et al*, 2008, 2009).

Although one of the well-described biochemical properties of αS is membrane binding associated with a structural switch, the biological function of the membrane-associated variant is unclear. Here, we demonstrate for the first time that αS inhibits fusion of model membranes. Biophysical studies led us to investigate the consequences of enhanced αS levels on membrane fusion *in vivo*. Life imaging in cultured cells and *Caenorhabditis elegans* demonstrates that expression of αS induces mitochondrial fragmentation, whereas down-regulation of αS leads to elongation of mitochondria. Strikingly, the mitochondrial phenotype caused by expression of αS could be rescued by coexpression of three recessive PD-associated genes, PINK1, parkin and DJ-1, but not the corresponding familial PD-associated mutants PINK1 G309D, and parkin Δ1–79 or by the synthetic mutant DJ-1 C106A (Waak *et al*, 2009).

Results

αS inhibits membrane fusion in vitro

We tested the effect of αS in several 'classic' fusion assays using protein-free model membranes. In our first protocol, we used small unilamellar vesicles (SUVs) consisting of dipalmitoyl-phosphatidylcholine (DPPC), which are known to fuse below the chain-melting temperature T_m, increasing their diameter from 30 to 70 nm (Schullery *et al*, 1980a, b; Gaber and Sheridan, 1982). This spontaneous fusion is a very slow process (Supplementary Figure S1). Trace amounts of non-ionic detergent $C_{12}E_8$ accelerate the fusion of DPPC-SUV, particularly at temperatures just below T_m (the gel to liquid–crystalline phase transition of bilayers of DPPC occurs at $T_m = 41^\circ C$). We measured vesicle fusion by following changes in the static light scattering. At 36°C a suspension of DPPC-SUV reached maximal light scattering values within 10 min after detergent addition (Figure 1A). Fusion was suppressed when the experiment was performed in the presence of increasing amounts of αS and was blocked completely at lipid/αS ratios $\leqslant$200 mole/mole (3 μM αS), that is at concentrations where αS binding to vesicles saturates (Nuscher *et al*, 2004). We also applied dynamic light scattering (DLS) experiments, which demonstrated the increase in diameter of fusing vesicles (Supplementary Figure S2). To confirm that the increase in light scattering of fusing vesicles was not an aggregation artifact, we used two fluorescent membrane fusion assays. In a lipid-mixing assay, NBD fluorescence of 'donor' vesicles was completely quenched prior to addition of detergent. Upon fusion of donor vesicles and vesicles without fluorescent probes, lipid mixing abolishes the quenching effect. Membrane fusion, monitored by this technique could be reduced by increasing amounts of αS (Figure 1B). Alternatively, in a contents-mixing assay we repeated the $C_{12}E_8$-induced fusion of DPPC-SUV by mixing equal amounts of vesicles with trapped Tb^{3+}-citrate with vesicles containing dipicholinic acid (DPA). Formation of the Tb^{3+}–DPA complex led to a strong increase in fluorescence (Figure 1C). Almost no fluorescence increase was observed after addition of αS at a lipid/protein molar ratio 200:1, indicating that fusion was effectively inhibited. Together, these independent experiments support the inhibition of membrane fusion by αS.

Considering the domain structure of lipid-bound αS, the question arises whether its anti-fusogenic behaviour is due to stabilization of packing defects in the bilayer (Kamp and Beyer, 2006), or rather to membrane repulsion caused by the negatively charged C-terminal domain. To distinguish between these two possibilities, the fusion assay was repeated using an αS mutant lacking the last 24 amino acids of the C-terminus. This fragment (αS1–116) was still capable of completely suppressing membrane fusion (Figure 1D). On the contrary, a peptide composed of 25 amino acids of the C-terminus of αS (αS116–140), as well as a peptide comprised of 25 amino acids of the centre region of αS (αS41–65), was not capable of inhibiting membrane fusion (Figure 1D). We also compared the anti-fusogenic effect of αS with other membrane-binding proteins. Cytochrome c and lysozyme have similar molecular weights as αS. Both are globular proteins with a net positive charge known to bind to membrane surfaces. Cytochrome c and lysozyme did not significantly slow down the fusion of DPPC-SUV (Figure 1E). Exchangeable apolipoproteins have structural similarities to αS and share stabilization of lipid packing because of the binding of a 'sided' helix to the lipid surface (Derksen *et al*, 1996; Nuscher *et al*, 2004; Cornell and Taneva, 2006; Beyer, 2007). Interestingly, apolipoprotein A-I (ApoA-I) blocked the fusion completely, just like αS (Figure 1E). These findings indicate that the folding and membrane interaction of the N-terminal domain rather than the negative charges of the C-terminal domain are responsible for the anti-fusogenic effect of αS.

To test whether the effect of αS also applies to vesicles composed of other lipids, we investigated fusion of vesicles composed of negatively charged palmitoyl-oleoyl-phosphatidylserine (POPS), triggered by Ca^{2+}-ions (Wilschut *et al*, 1980). Fusion was initiated by adding $CaCl_2$ and was complete within 10 min after the addition (Figure 1F). When αS was added after the addition of Ca^{2+}, the fusion rate was reduced >10 times. Again, we compared the anti-fusogenic effect of αS with other membrane-binding proteins. In this case, we used cytochrome c and poly-lysine. Poly-lysine, like cytochrome c, is expected to bind to negatively charged membranes (Zhang and Rowe, 1994). Cytochome c had no effect even at a 10-fold higher molar concentration than αS. Poly-lysine reduced the fusion rate about five times (Figure 1F). Having established the suppression of membrane fusion by αS in classic fusion assays of vesicles composed of only one kind of lipid, we wondered whether αS would also suppress fusion of membranes of lipid mixtures mimicking compositions of biological membranes. The effect of αS on polyethyleneglycol (PEG)-mediated fusion of vesicles composed of a lipid mixture with reported optimal fusion potential (Haque *et al*, 2001) is shown in Figure 1G. The suppression of fusion by αS was significant, although higher amounts of αS were required compared with the DPPC-SUV and POPS-SUV, probably because of a lower affinity of αS to

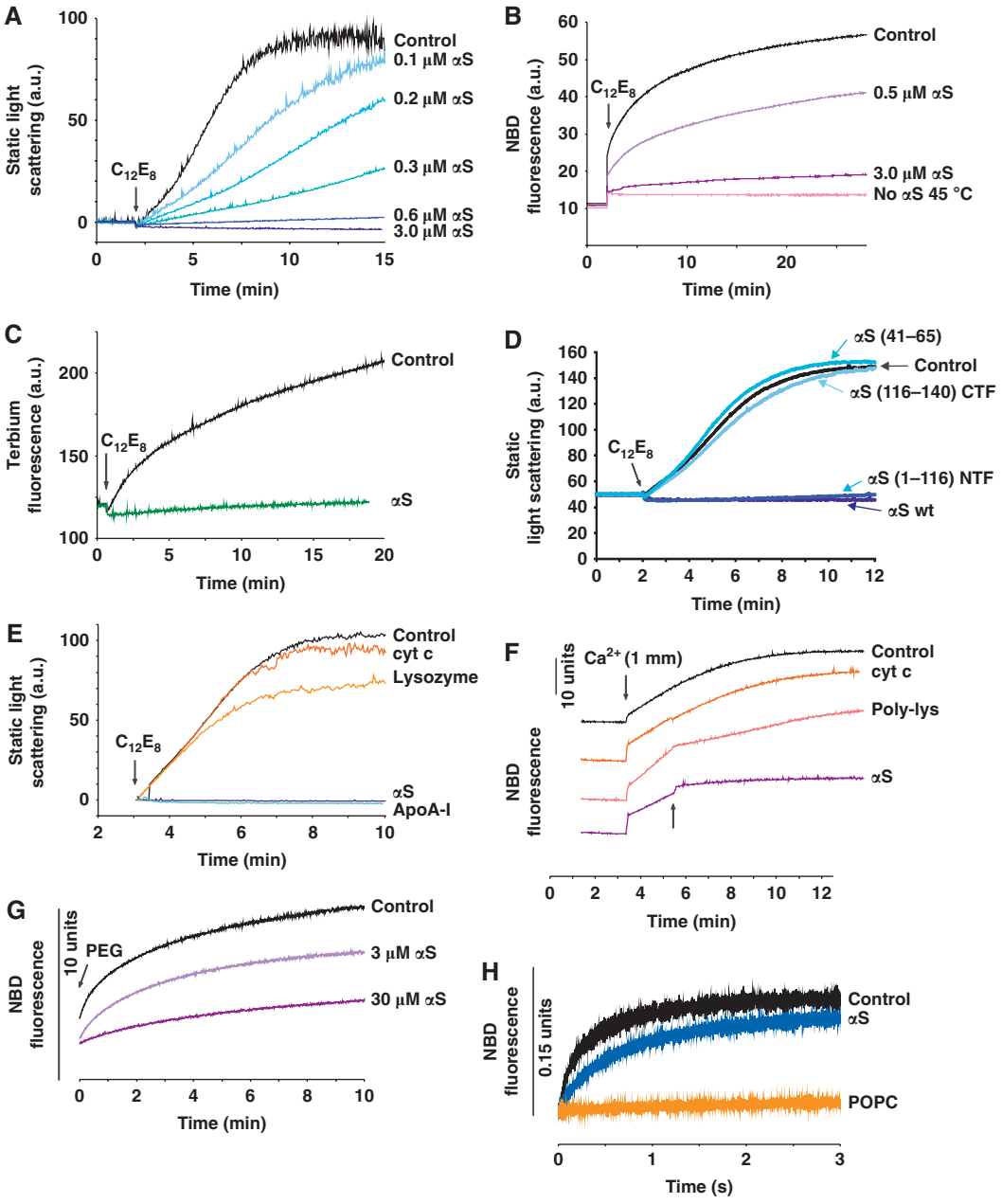

Figure 1 αS inhibits membrane fusion *in vitro*. (**A**) Fusion of DPPC-SUV was monitored by the increase in static light scattering upon addition of an aliquot of $C_{12}E_8$. Increasing amounts of αS inhibit membrane fusion (blue lines). Lipid concentration 600 μM, $T = 36°C$. (**B**) Lipid-mixing assay of DPPC-SUV. αS inhibited fusion completely at lipid/αS = 200 mole/mole (purple line). $T = 35°C$. Pink line: no fusion occurred at 45°C, that is at temperature above T_m. (**C**) Contents-mixing assay carried out in the presence and absence of αS (lipid/αS = 200 mole/mole, green line). $T = 30°C$. (**D**) An N-terminal fragment mutant of αS, αS(1–116) (blue line), lacking the negatively charged C-terminal domain was capable of completely suppressing the fusion of DPPC-SUV, like wt-αS (dark blue line); whereas peptides comprised of the C-terminal fragment, αS(116–140), or the central domain of αS, αS(41–65), failed to inhibit fusion (blue lines). Lipid/protein = 100 mole/mole. $T = 25°C$. (**E**) Comparison of inhibition of membrane fusion by αS with cytochrome c, lysozyme and Apolipoprotein A-I (ApoA-I). For all proteins: lipid/protein = 200 mole/mole. $T = 36°C$. (**F**) Ca^{2+}-induced fusion of POPS-SUV. Fusion was initiated by adding an aliquot of $CaCl_2$ and monitored by the lipid-mixing assay. αS, added 2 min after the addition of Ca^{2+} (arrow), blocked fusion almost completely (lipid/αS = 200 mole/mole). Control experiments: cytochrome c (lipid/protein = 20 mole/mole) or poly-lysine (lipid/protein 200 mole/mole) was added instead of αS. $T = 25°C$. (**G**) SUV of a mixture of lipids with reported optimal fusion potential (DOPC/DOPE/BBSM/cholesterol, 35:30:15:20 molar ratio) (Haque *et al*, 2001). Fusion was initiated by addition of 4% PEG and followed using the lipid-mixing assay. Total lipid concentration was 300 μM. When the experiment was repeated with αS, fusion was slowed. $T = 37°C$. (**H**) Spontaneous rapid fusion of SUV composed of lipids with opposite charges (POPS-SUV and PC^+-SUV). Lipid-mixing assay performed in stop-flow fluorimetry. Lipid concentration was 60 μM. αS (1.2 μM) inhibited the fusion. When POPS was replaced by POPC (uncharged) no fusion occurred, as expected. $T = 25°C$.

the membranes comprised of the chosen lipid mixture. Finally, rapid spontaneous fusion can be achieved upon mixing of vesicles with opposite interfacial net charges (Pantazatos and MacDonald, 1999; Lei and MacDonald, 2003). In this assay, fusion was complete after about 3 sec (Figure 1H). Again fusion was reduced by αS. Taken together, these findings demonstrate that αS selectively blocks membrane fusion in a number of independent *in vitro* fusion assay systems.

αS impairs mitochondrial fusion in cultured cells

Mitochondria change their morphology because of continuous fusion and fission (Detmer and Chan, 2007; Westermann, 2008). In addition, mitochondrial morphology and function is affected by loss of parkin or PINK1 function, which are both associated with familial PD (Kitada *et al*, 1998; Valente *et al*, 2004; Exner *et al*, 2007; Dagda *et al*, 2009; Lutz *et al*, 2009; Morais *et al*, 2009; Sandebring *et al*, 2009). To prove whether enhanced levels of αS, as observed in sporadic PD (Sharon *et al*, 2003; Chiba-Falek *et al*, 2006; Grundemann *et al*, 2008) as well as in familial PD associated with a triplication of the αS gene (Singleton *et al*, 2003), influence the balance between mitochondrial fission and fusion, we overexpressed αS in neuronal SH-SY5Y cells. This was particularly interesting as αS has been reported to bind to intracellular membranes including mitochondria (Nakamura *et al*, 2008; Shavali *et al*, 2008). Changes in mitochondrial morphology were monitored by imaging of cells, transfected with mito-GFP. When wild-type αS was overexpressed in SH-SY5Y cells, increased mitochondrial fragmentation was observed (Figure 2A). Quantification of the relative amounts of cells with fragmented mitochondria revealed that upon overexpression of αS, the number of cells that display fragmented mitochondria increased from 34% under control conditions to 46% (Figure 2B). Expression of similar amounts of mutant αS-A30P or A53T led to fragmentation of mitochondria to the same extent as the wild-type protein (Figures 2A–C). This is consistent with the finding that mutants of αS also bind to model membranes (Nuscher *et al*, 2004; Ramakrishnan *et al*, 2006; Giannakis *et al*, 2008; Karpinar *et al*, 2009; Perlmutter *et al*, 2009). β-Synuclein (βS) shares a number of biological and biophysical properties with αS, including binding to lipid surfaces (Nuscher *et al*, 2004; Beyer, 2007). We therefore investigated if βS may also affect mitochondrial fusion/fission. Indeed, both orthologs lead to the formation of fragmented mitochondria (Figures 2D–F), suggesting a redundant function of αS and βS.

To further address the question whether the increase in mitochondrial fragmentation observed in αS-expressing SH-SY5Y cells is due to alterations in mitochondrial fusion, we performed a PEG fusion assay (Niemann *et al*, 2005; Malka *et al*, 2007) (Figure 3). A first set of cells was transiently cotransfected with mito-GFP and αS or empty vector as a control. Another set of cells was cotransfected with mito-DsRed and αS or vector. At 8 h after transfection, both sets of cells were mixed and plated on coverslips. After 16 h, fusion of cocultured cells was induced by a 90-s treatment with PEG and fused cells were further incubated in the presence of cycloheximide for 5 h. Mitochondria of fused cells were analysed by confocal microscopy. Mitochondrial fusion is indicated by extensive colocalization of mito-GFP and mito-DsRed in control cells (Figures 3A and B). In contrast, upon overexpression of αS colocalization was dramatically reduced demonstrating that αS blocks mitochondrial fusion.

Mitochondria are known to fragment in stress situations (Westermann, 2008; Cho *et al*, 2010). To exclude that the changes in mitochondrial phenotype caused by αS overexpression are due to a secondary stress response, we performed control experiments to prove whether mitochondrial function was impaired by the expression of αS. The membrane potential in SH-SY5Y cells expressing mito-GFP was evaluated by TMRM fluorescence intensity of the mitochondria. There was no difference in TMRM fluorescence intensity when we compared the vector control cells with cells expressing αS (Figures 4A and B). In addition, no reduction of ATP production was observed in cells expressing wt-αS, αS A30P or αS A53T compared with the control-transfected cells (Figures 4C and D).

αS enhances age-dependent mitochondrial fragmentation in C. elegans

In line with our observations in cultured cells, when expressed in *C. elegans* body wall muscles (BWMs) wt-αS led to dramatic alterations of mitochondrial morphology and also to mitochondrial fragmentation (Figure 5). As *C. elegans* BWMs contain a highly stereotyped planar arrangement of mitochondria (Figure 5A) they are particularly suited for the analysis of mitochondrial morphology. To visualize mitochondria, we used the transmembrane domain of the outer mitochondrial membrane protein TOM70 fused to CFP (Labrousse *et al*, 1999). Moderate expression of αS led to the formation of extremely thin and highly interconnected mitochondria (Figures 5B and D) in about 20–40% of the transgenic BWMs. However, the majority, 50–70% of αS-expressing BWMs contained highly fragmented mitochondria that are roundish in their appearance (Figures 5C and D) in all independent transgenic strains analysed. Strikingly, a similar mitochondrial fragmentation was observed in aged 7-day-old worms in the absence of exogenous αS expression (Figure 5E), suggesting that mitochondrial fragmentation also happens during the normal ageing process of the BWM tissue. *C. elegans* BWMs are particularly susceptible to ageing and have been shown to gradually and progressively deteriorate with age (Herndon *et al*, 2002). *C. elegans* mean life span is about 12–18 days. After reaching adulthood, *C. elegans* hermaphrodites lay all their eggs within approximately 3 days and then persist through a post-reproductive period were senescent decline is evident (Herndon *et al*, 2002). As *C. elegans* animals still grow after reaching adulthood, aged BWMs were bigger in size (Figure 5E). Interestingly, ectopic expression of αS accelerated the mitochondrial aging phenotype (Figures 5E and F).

αS expression also led to mitochondrial fragmentation in neurons (Figures 5G–I). In neuronal cell bodies, we distinguished three categories of mitochondrial morphology: ring-like [R], tubular [T] or fragmented [F] mitochondria. Wild-type neurons mostly contained ring-like and long tubular mitochondria, whereas αS-expressing neurons showed mostly fragmented mitochondria. These observations confirmed that αS expression in living organisms leads to mitochondrial fragmentation in a tissue-independent manner.

αS is enriched at the mitochondrial outer membrane

To assess whether the increased mitochondrial fragmentation seen upon αS overexpression is caused by a direct binding of αS to mitochondrial membranes, we analysed mitochondrial morphology and the subcellular localization of αS by high pressure freeze (HPF) immuno-electron microscopy (EM). We did not observe any changes in the morphology of the mitochondrial cristae by αS expression as seen in the HPF-EM images (Figure 6A). We detected αS by using polyclonal αS antibodies on 90 nm thin immuno-EM sections of plastic embedded and HPF fixed SH-SY5Y cells. Label density was

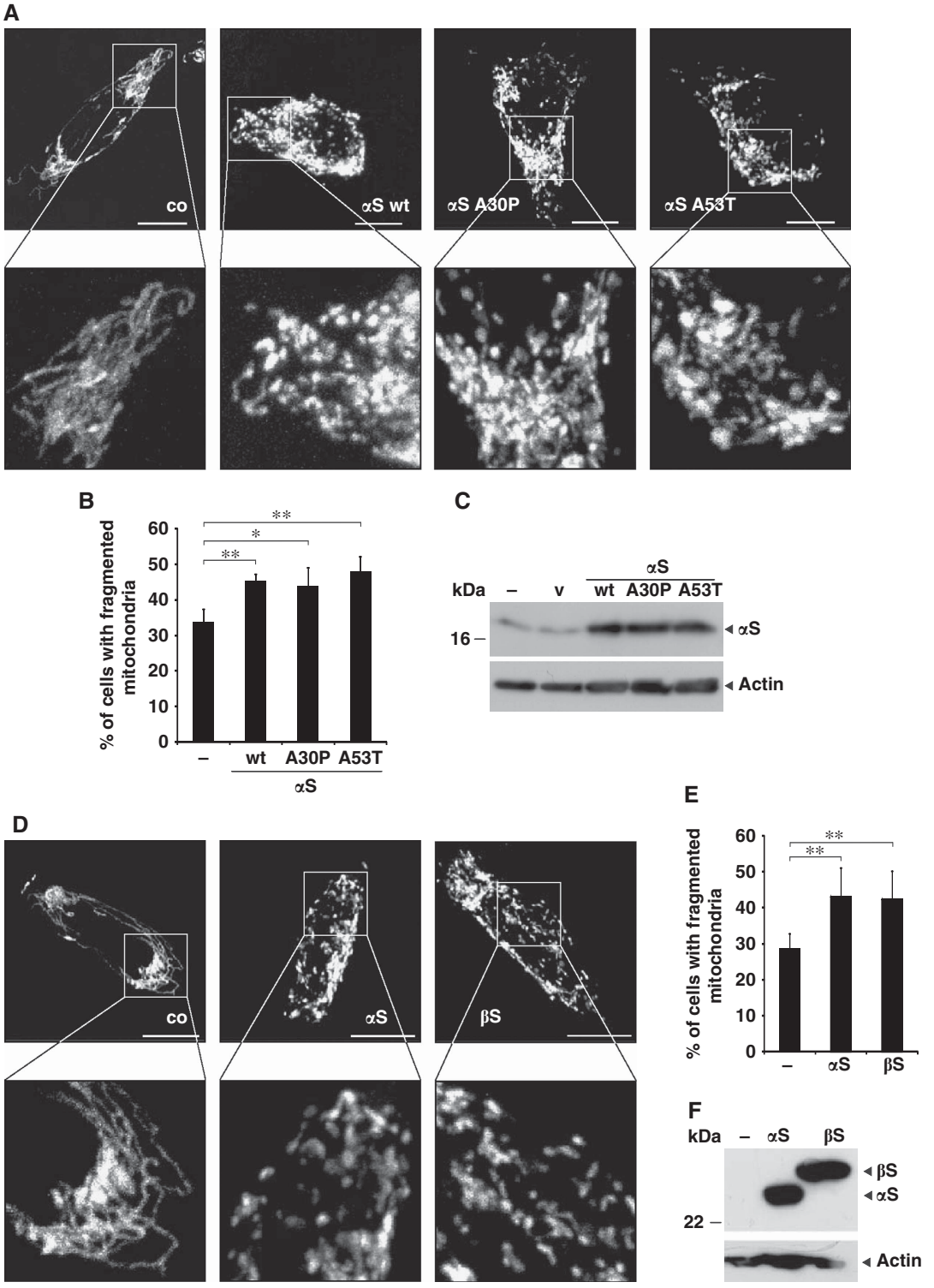

Figure 2 Mitochondrial fragmentation imaged in SH-SY5Y cells expressing αS. (**A**) Images of fluorescently labelled mitochondria. The panels display representative individual cells either control transfected (co) or transfected with wild-type αS (αS-wt), αS A30P or αS A53T. Scale bars = 10 μm. (**B**) Statistical analyses of mitochondrial morphology of cells from the experiments shown in (**A**). Approximately 250 cells of each experiment were counted, and the relative amount of transfected cells with altered mitochondrial morphology (i.e. fragmentation) was determined. (**C**) Expression levels of αS were analysed by western blotting using β-actin as loading control (v, vector). (**D**) Images of fluorescently labelled mitochondria. The panels display representative individual cells either untransfected (co) or transfected with αS-V5 (αS) or β-synuclein-V5 (βS). Scale bars = 10 μm. (**E**) Statistical analyses of mitochondrial morphology of cells from the experiments shown in (**D**). Approximately 300 cells of each experiment were counted, and the relative amount of transfected cells with altered mitochondrial morphology (i.e. fragmentation) was determined. Error bars indicate s.d. (**F**) Expression levels of αS and βS were analysed by western blotting with a V5-antibody using β-actin as loading control. $^{*}P \leqslant 0.05$, $^{**}P \leqslant 0.01$.

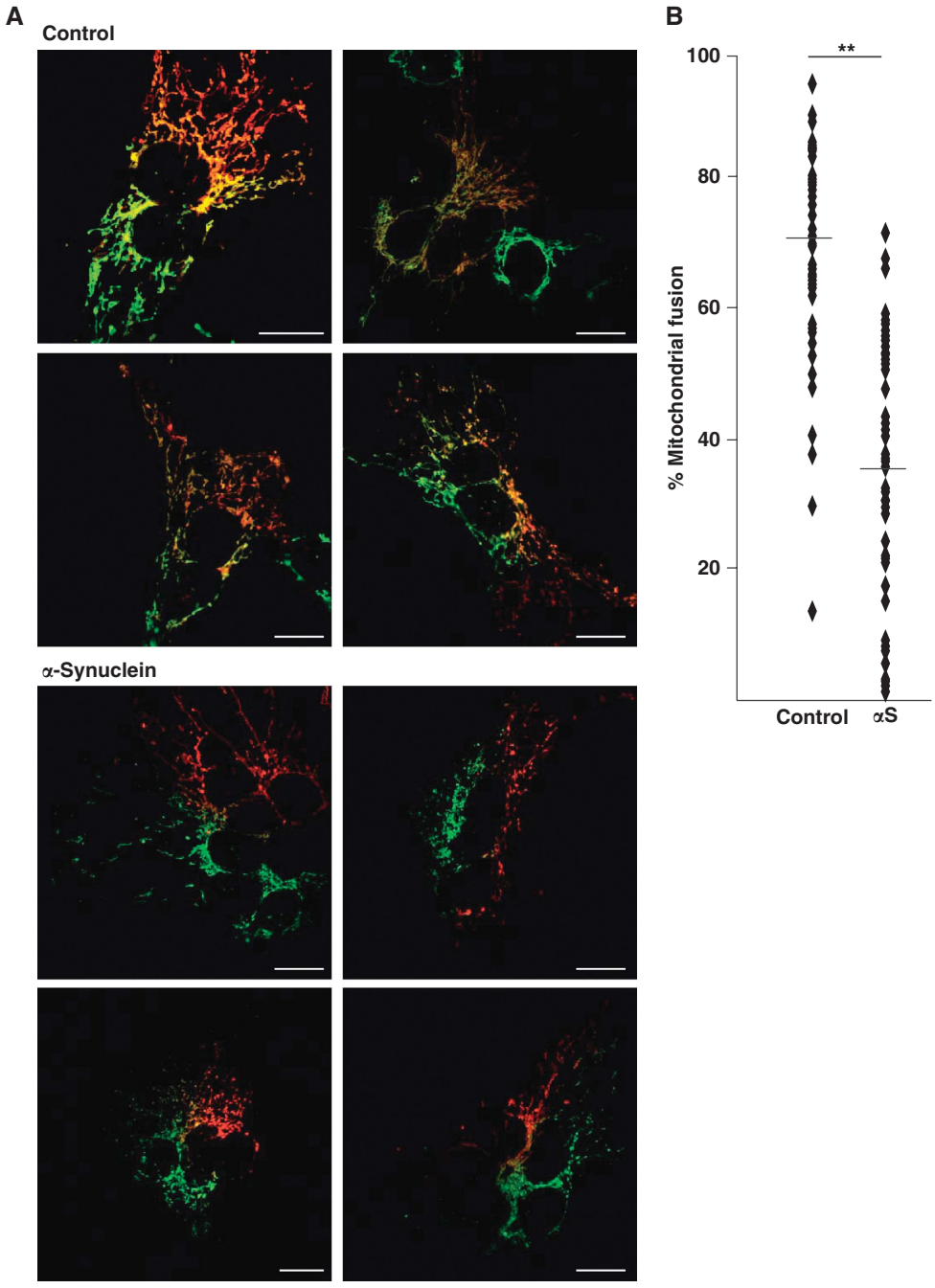

Figure 3 αS decreases fusion of differentially labelled mitochondrial populations. Cells expressing mito-GFP or mito-DsRed were fused with PEG in the presence or absence of exogenous αS. (**A**) Confocal images of representative polykaryons are shown. Fusion was monitored by the extent of mito-GFP and mito-DsRed colocalization. Scale bars = 15 μm. Upper panel: vector transfected (control); lower panel: αS transfected. (**B**) Quantification of mitochondrial fusion in αS and control cells. Each dot represents one measured value. Mean values are indicated by horizontal bars. Asterisks indicate significant differences in the percentage of cell hybrids with fused mitochondria compared with the vector control. Expression controls are provided in Supplementary Figure S3.

estimated by calculating the number of gold particles per μm^2 of the EM image. Three different areas were measured: the cytosol, the inside of mitochondria and the mitochondrial membrane. The mitochondrial membrane area was calculated as length of the membrane (μm) multiplied with 0.03 μm, because of possible shift of the gold particle of 15 nm in both directions of the membrane (Hoppert, 2003). When αS was overexpressed, it was detected at the mitochondrial membrane, whereas no αS signal was found inside mitochondria (Figures 6B and C). The amount of αS bound to the mitochondrial membrane was evaluated statistically (Figure 6C). About 38 gold particles were detected per μm^2 mitochondrial membrane area, whereas less than one αS signal was detected per μm^2 of cytosol. Because of the fact that HPF immuno-EM is a post-embedding labelling technique, the labelling intensity is usually lower than with classical fixation pre-embedding techniques. Therefore, endogenous αS was near the detection limit. These findings suggest that αS induces mitochondrial fragmentation by direct binding to the outer mitochondrial membrane.

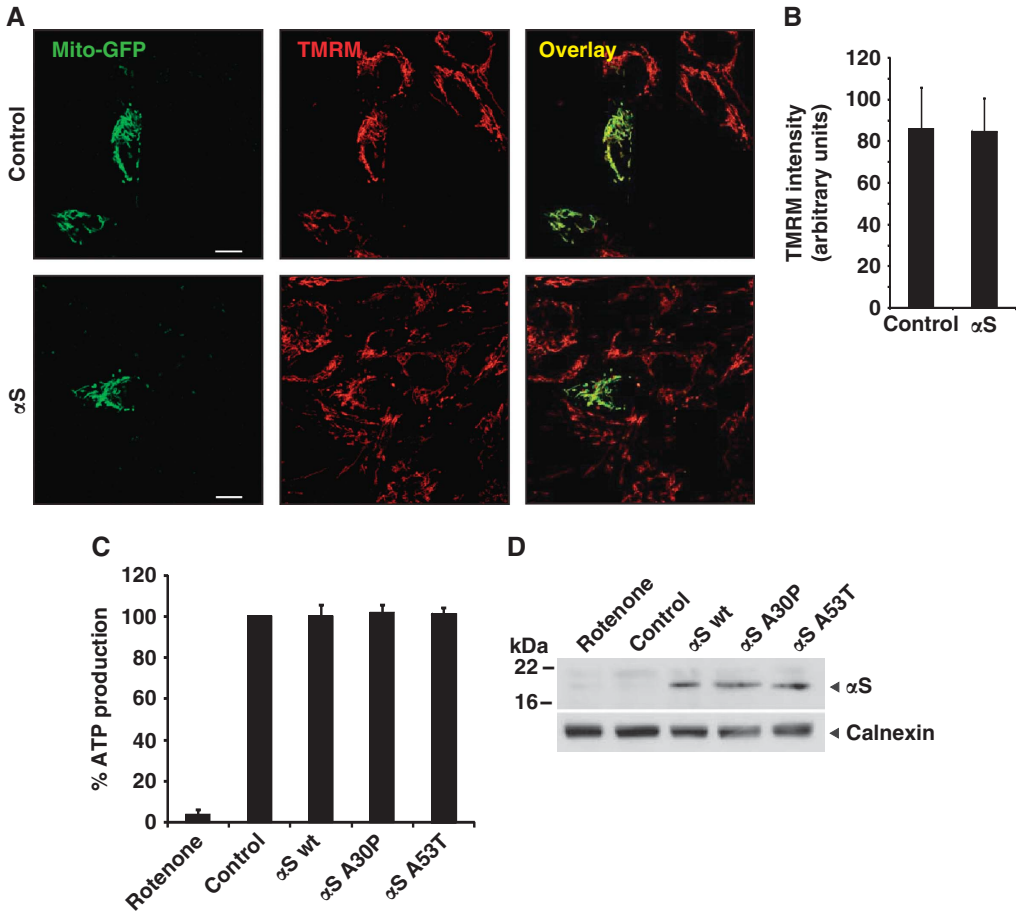

Figure 4 Mitochondrial function is not impaired by low level expression of αS. (**A**) SH-SY5Y cells were cotransfected with mito-GFP and vector (control) or αS. Living cells were stained with TMRM and colocalization was determined by overlay. (**B**) Quantification of TMRM fluorescence intensity. For each condition, $n = 30$ pictures as shown in (**A**) were quantified. (**C**) Steady-state cellular ATP levels were measured in SH-SY5Y cells transfected with either vector (control), αS wt, αS A30P or αS A53T. (**D**) Expression levels of αS were analysed by western blotting using calnexin as loading control. Error bars indicate s.d.

Pink-1, parkin and DJ-1 rescue αS-induced changes in mitochondrial morphology

Previously it was shown that familial PD-associated genes can confer stress protection (Palacino *et al*, 2004; Clark *et al*, 2006; Park *et al*, 2006). We therefore investigated whether Pink-1, parkin and DJ-1 protect from αS-induced mitochondrial fragmentation. Strikingly, coexpression of wild-type PINK1, wild-type parkin, wild-type DJ-1 with αS rescued the morphological phenotype caused by αS (Figure 7A). However, the mitochondrial fragmentation caused by αS overexpression could not be rescued by coexpression of the familial PD-associated mutants PINK1 G309D or by a parkin mutant lacking the N-terminal ubiquitin-like domain (Δ1–79), which is impaired in its ubiquitylation activity and neuroprotective capacity (Henn *et al*, 2007). The synthetic loss of function DJ-1–1 C106A mutant that prevents oxidation at the active centre (Waak *et al*, 2009) also failed to rescue the mitochondrial fragmentation (Figure 7A). Expression of wild-type PINK1, wild-type parkin and wild-type DJ-1 and each mutant alone did not affect mitochondrial morphology (Figure 7B).

Downregulation of αS forces mitochondrial fusion

To further substantiate the physiological relevance of the involvement of αS in modulating mitochondrial morphology, we used a siRNA knockdown approach to study physiological consequences of αS loss-of-function. As αS binds to mitochondria (Figure 6) (Li *et al*, 2007; Cole *et al*, 2008; Devi *et al*, 2008; Nakamura *et al*, 2008; Parihar *et al*, 2008), we assumed that a loss of αS may lead to the opposite effect as observed upon overexpression, namely to an increase of cells with elongated mitochondria (Figure 8). Knockdown of αS by siRNA considerably reduced αS protein levels (Figure 8C). Under these conditions, a significant increase in the number of cells with elongated mitochondria (13%) was observed (Figures 8A and B). Mitochondrial tubules were extended through the entire cell, which was rarely observed in control transfected (4%) or untransfected cells. Expression of siRNA resistant αS reverted this phenotype to control levels (5%), demonstrating the specificity of the knockdown effect. In these experiments, mitochondrial morphology was monitored using the fluorescent dye DiOC6(3). Similar results were obtained when we imaged mitochondria labelled with mito-GFP (Supplementary Figure S5).

To independently confirm that αS suppresses mitochondrial fusion, we induced fragmentation via the addition of the respiratory chain uncoupler CCCP (Ishihara *et al*, 2003). After 1 h, CCCP was removed and the recovery of mitochondrial morphology was monitored over the next 45 min in the presence of endogenous αS or upon siRNA-mediated

knockdown of αS. After CCCP treatment, the number of mitochondria with normal morphology was dramatically reduced (Figure 8D). Over the next 45 min in the absence of CCCP physiological mitochondrial morphology recovered significantly faster upon reduction of αS as in the presence of normal αS levels. Similarly, the amount of fragmented mitochondria dramatically increased during the 1-h treatment with CCCP. The number of fragmented mitochondria then

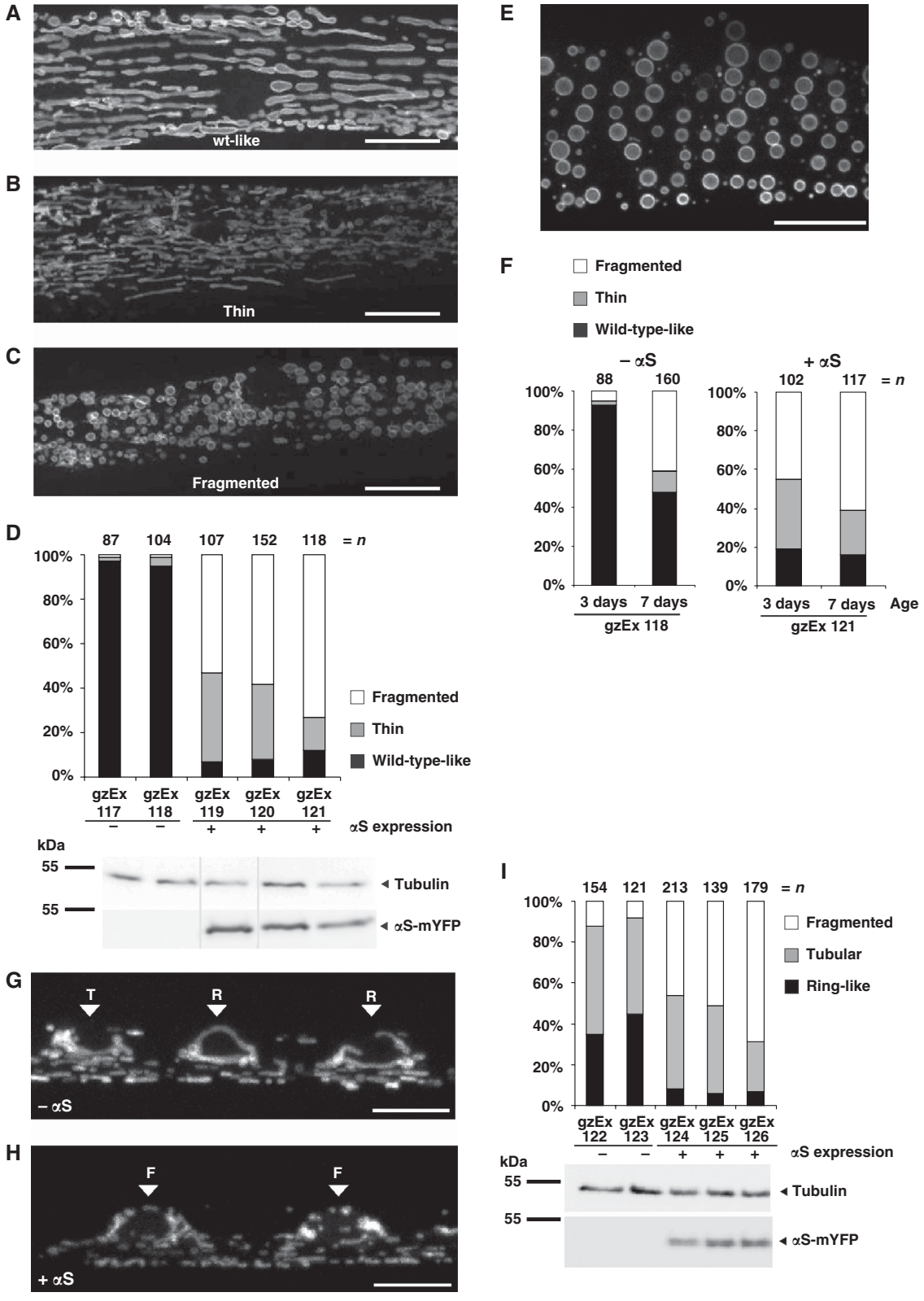

declined significantly faster in cells with reduced αS levels. These findings therefore further support that αS directly inhibits mitochondrial fusion.

αS-mediated mitochondrial fragmentation is independent of mitochondrial fusion and fission proteins

We next shifted the dynamic equilibrium of mitochondria towards increased fusion and investigated whether this can be antagonized by addition of αS. This was done on the one hand by expression of the fusion-promoting proteins Mfn1, Mfn2 and Opa1 or on the other hand by downregulation of the fission-promoting protein Drp1. Overexpression of αS did not affect expression levels or subcellular localization of Mfn1, Mfn2, Opa1 or Drp1. Furthermore, no aberrant processing of Opa1 was observed (Duvezin-Caubet *et al*, 2006) (Supplementary Figure S7). Nevertheless, the appearance of a higher number of cells with elongated and highly connected mitochondria, as observed upon expression of Mfn1, Mfn2 or Opa1 alone was reduced by coexpression of αS (Figure 9A). Moreover, expression of Mfn2 together with the downregulation of αS had an additive effect in inducing mitochondrial elongation (Figure 9B). Likewise, knockdown of Drp1 with siRNA leads to an increase in elongated mitochondria, indicating reduced mitochondrial fission. This increase was significantly less when αS was overexpressed. Similarly, elongation of mitochondria was induced by expression of the dominant-negative Drp1 K38E mutant. Again, coexpression with αS reduced the number of cells with elongated mitochondria (Figures 9C and D).

Discussion

Familial PD is not only caused by missense mutations within the αS gene, but also by a gene duplication/triplication, which leads to enhanced protein levels of αS (Singleton *et al*, 2003; Ibanez *et al*, 2004). Moreover, in patients with sporadic PD, an increase of αS mRNA and oligomers was observed (Sharon *et al*, 2003; Chiba-Falek *et al*, 2006; Grundemann *et al*, 2008). A polymorphism in the SNCA promoter increases gene expression and PD susceptibility (Maraganore *et al*, 2006). Two recent large genome-wide association studies concordantly revealed that common variants in SNCA increase the risk of PD (Satake *et al*, 2009; Simon-Sanchez *et al*, 2009). αS has a high propensity to bind to lipid membranes *in vitro* and multiple evidence exists that αS may affect vesicular trafficking, Golgi structure and mitochondrial function, although a unifying cellular mechanism behind these observations is not known (Cooper *et al*, 2006; Fujita *et al*, 2006; Larsen *et al*, 2006; Gitler *et al*, 2008; Parihar *et al*, 2009). On the basis of biophysical studies, our hypothesis has been that αS inhibits membrane fusion. Undoubtedly, proteins and Ca^{2+} ions have an essential role in the regulation, targeting and triggering of fusing membranes *in vivo* (Weber *et al*, 1998; Nickel *et al*, 1999; Tamm *et al*, 2003; Liu *et al*, 2005; Chen *et al*, 2006; Dennison *et al*, 2006; Takamori *et al*, 2006). However, a necessary requirement for any membrane fusion is *mixing of the lipids* (Chernomordik *et al*, 1995; Chernomordik and Kozlov, 2003; Lentz, 2007; Weinreb and Lentz, 2007; Piomelli *et al*, 2007). High curvature of membranes causes defects in the packing of the lipids, which are necessary to trigger the formation of a fusion stalk (Chernomordik *et al*, 1995; Dennison *et al*, 2006). As αS seals defects in stressed bilayers (Kamp and Beyer, 2006), we expected that αS might inhibit membrane fusion (see model in Figure 10). Although we recognize that the *in vitro* fusion assays do not fully represent *in vivo* membrane fusion events, the biophysical experiments provided the basis for the *in vivo* experiments. We therefore first studied the influence of αS binding to lipid vesicles *in vitro* and in a next step investigated the effects of αS expression in the living cell and in an animal model. In this study, αS inhibited fusion in all *in vitro* fusion assays applied. Differential scanning calorimetry experiments further supported our hypothesis that αS suppresses fusion due to its unique interaction with the membrane (Supplementary Figure S1). In control experiments, no significant decrease in the fusion rate was found with cytochrome c and lysozyme. Thus, partial coating of the lipid/water interface by proteins with a net positive charge affected the fusion only marginally. Poly-lysine inhibited fusion but to a much lesser extent compared with αS. One poly-lysine molecule contains about 500 lysine residues. At the lipid/protein molar ratio used, a large fraction of the outer surface would be coated by poly-lysine. In this case, the fusion would be inhibited by charge repulsion. In contrast, ApoA-I inhibited fusion as efficiently as αS. As the biological function of apolipoproteins is to stabilize plasma lipoproteins (Gursky, 2005; Cornell and Taneva, 2006), we conclude that ApoA-I suppresses fusion of membranes probably by a similar mechanism as αS. Finally, fusion was also blocked with a truncated αS, lacking the charged C-terminal domain. These observations support our hypothesis that αS inhibits membrane fusion by stabilizing the lipid packing of stressed bilayers, independently of other protein factors that might be involved in the fusion machinery of membranes.

Investigating *in vivo* effects of αS on mitochondrial fusion was particularly interesting, as morphological changes and

Figure 5 αS expression leads to mitochondrial fragmentation in *C. elegans* muscles and neurons. (**A**) In wild-type muscles without expression of αS, mitochondria are forming regular tubular structures. (**B**, **C**) Expression of human αS leads to changes in mitochondrial morphology, which can be classified into two categories: (**B**) very thin and highly interconnected tubules and (**C**) fragmented vesicular mitochondria. Scale bars = 10 μm. (**D**) Quantification of the relative appearance of wild-type-like, fragmented, and thin mitochondria in independent transgenic lines expressing αS-mYFP. Expression levels of αS-mYFP were analysed by western blot using tubulin as a loading control. All lanes originate from the same gel. Only the lanes of those transgenic lines, which were chosen for imaging due to good penetrance and fluorescent signal, are shown here. (**E**) Mitochondrial fragmentation is also observed in aged 7-day-old wild-type body wall muscles. Scale bar = 10 μm. (**F**) Mitochondrial morphologies are compared between 3 day versus 7-day-old muscles without (right graph) and with αS-mYFP expression (left graph). (**G**, **H**) Images show TOM70-CFP-labelled mitochondria in motoneurons of young adult *C. elegans*. Arrowheads label neuronal cell bodies, indicating the morphological category. The mitochondrial morphology in neuronal cell bodies was grouped into three categories: ring-like [R], tubular [T] or fragmented [F] mitochondria. Wild-type neurons mostly contain ring-like and long tubular mitochondria (**G**), whereas αS-expressing neurons show mostly fragmented mitochondria in cell bodies as well as in the axons (**H**). Scale bars = 5 μm. (**I**) Quantification of relative occurrence of ring-like, tubular and fragmented mitochondria and αS-mYFP expression levels.

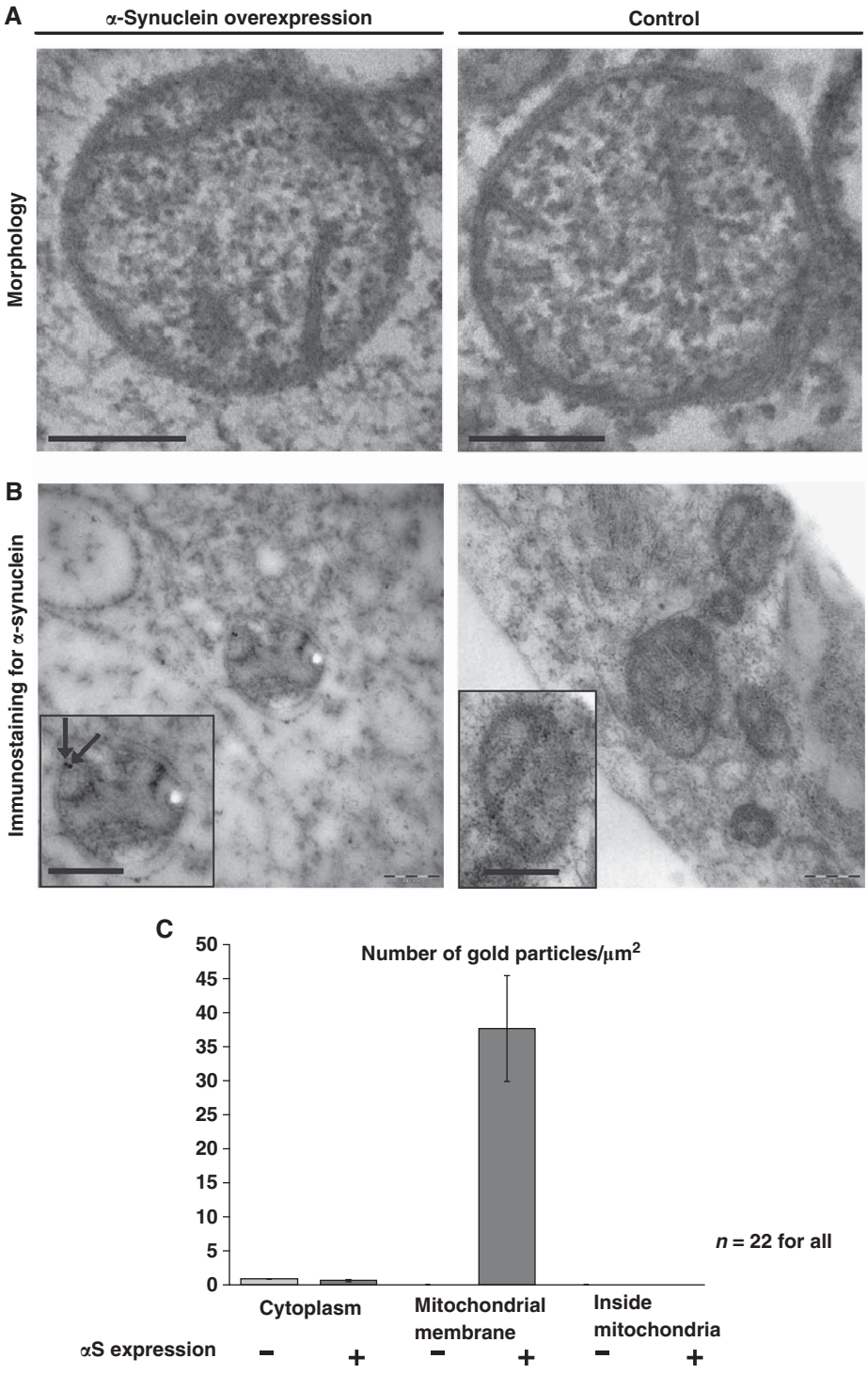

Figure 6 αS binds to mitochondrial outer membranes. (**A**) Electron microscopy of mitochondria in cells overexpressing αS (left panel) and without overexpression (control, right panel). Scale bars = 200 nm. (**B**) Immunostaining for αS. Insets: Mitochondria in high magnification. Arrows indicate localization of αS. Scale bars = 200 nm. (**C**) Statistical analysis of the density of immunogold labelling in the cytosol, at the mitochondrial membrane and inside the mitochondria, comparing αS overexpressing cells (+) and the control without overexpression (−). No label inside the mitochondria was detected in both samples. Error bars indicate s.d.

dysfunction of mitochondria have frequently been reported as a consequence of a loss of function of familial PD-associated genes such as PINK1 and parkin (Exner *et al*, 2007; Dagda *et al*, 2009; Lutz *et al*, 2009; Sandebring *et al*, 2009). Moreover, localization of αS to mitochondria has also been reported (Li *et al*, 2007; Cole *et al*, 2008; Devi *et al*, 2008; Nakamura *et al*, 2008; Parihar *et al*, 2008) and was confirmed in this study. We found evidence that αS is functionally involved in fusion of mitochondrial membranes. This was demonstrated by different approaches: (i) when cells were transfected with αS, a significantly larger amount of the cells displayed fragmented mitochondria (Figure 2). Similarly,

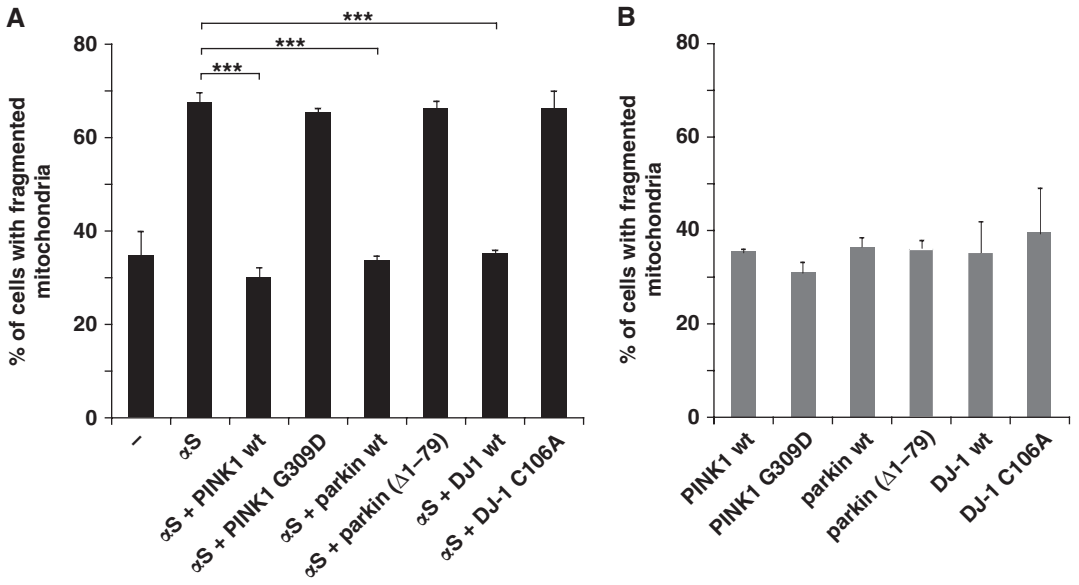

Figure 7 Expression of three familial PD-associated genes rescues mitochondrial fragmentation caused by αS. (**A**) Coexpression of PINK1, parkin or DJ-1 with αS rescues fragmentation of mitochondria, whereas their loss-of-function mutants do not. Cells were transfected as indicated and mitochondrial morphology was quantitated as in Figure 2B. (**B**) Single expression of PINK1, parkin or DJ-1 or each mutant alone does not affect mitochondrial morphology. Error bars indicate s.d. Expression controls are provided in Supplementary Figure S4. ***$P \leqslant 0.001$.

increased fragmentation of mitochondria was observed, when αS was expressed in BWMs and neurons of *C. elegans* (Figure 5). Interestingly, overexpression of αS accelerated a mitochondrial phenotype associated with physiological aging (Figure 5). As aging is a major risk factor for PD, this finding may have fundamental implications for the understanding of disease progression. (ii) The opposite phenotype, namely an elongation of mitochondria, occurred upon siRNA-mediated knockdown of αS (Figure 8). (iii) The experiment from Figure 8D showed that re-elongation of mitochondria upon CCCP-induced fragmentation was faster when αS levels were suppressed by αS siRNA. (iv) Specific enrichment of αS at mitochondrial outer membranes was visualized by immuno-EM. Notably, under conditions of mitochondrial fragmentation, cristae structure and length was unchanged and morphology was not affected on the level of EM. These experiments support the idea that αS binds to the outer membrane of mitochondria and inhibits or reduces their fusion. (v) When the plasma membranes of two populations of cells with differently coloured mitochondria were fused, subsequent mitochondrial fusion was significantly reduced when αS was overexpressed (Figure 3). (vi) When fusion was elevated by overexpression of the fusion-promoting proteins Mfn1, Mfn2 and Opa1, by downregulation of the fission-promoting protein Drp1 or by expression of the dominant-negative mutant Drp1-K38E, we observed a backshift of the equilibrium towards reduced fusion by coexpression of αS. Together, these data indicated that αS is not interacting directly with proteins involved in fusion or fission machineries. We propose that the influence of αS on mitochondrial dynamics is based on its interaction with membrane lipids, preventing the necessary formation of a fusion stalk, an idea that is strongly supported by our *in vitro* fusion experiments. Moreover, αS could inhibit lipid fusion events in protein-assisted mitochondrial fusion.

An alternative explanation for the observed effects of αS on mitochondrial dynamics would be that αS enhances mitochondrial fission. This is unlikely as the free-energy change involved with the structural switch of αS upon membrane binding (Nuscher *et al*, 2004) is not enough to cause fission and mitochondrial fission is a GTP requiring event (Westermann, 2008). The experiment of Figure 3, in which fusion of red and green labelled mitochondria in fused cells was slower when αS was overexpressed, can only be explained by an inhibitory effect of αS on fusion. Furthermore, the experiment from Figure 8D showed that re-elongation of mitochondria upon CCCP-induced fragmentation was faster when cytosolic αS levels were suppressed by αS siRNA. As during the re-elongation phase hardly any mitochondrial fission occurs, the slower re-elongation in the presence of αS can only be explained by a specific inhibitory effect of αS on the fusion of mitochondrial membranes. Another alternative explanation for the observed effects of αS on mitochondrial dynamics would be that αS expression alters the levels of expression of fission or fusion proteins, their subcellular localizations and/or post-translational modifications. However, no such effects were observed (Supplementary Figure S7).

We suggest that αS may have a general protective role preventing spontaneous membrane fusion. A rather unselective lipid membrane binding of αS independent of the individual fusion machineries suggests a pleiotropic function of αS. Indeed, there is evidence that αS directly affects Golgi morphology as well as priming of synaptic vesicles (Gosavi *et al*, 2002; Fujita *et al*, 2006; Larsen *et al*, 2006). Interestingly, a recent genome-wide screen for yeast genes that rescue αS-mediated toxicity revealed several conserved genes involved in vesicular trafficking including the evolutionarily conserved Rab1 GTPase Ypt1 (Cooper *et al*, 2006). In subsequent experiments, the authors were also able to show that Rab1 overexpression in the model systems *C. elegans* and *Drosophila melanogaster* were similarly effective to ameliorate αS-induced cellular toxicity. In combination with *in vitro* ER-to-Golgi transport assays, this strongly indicates that

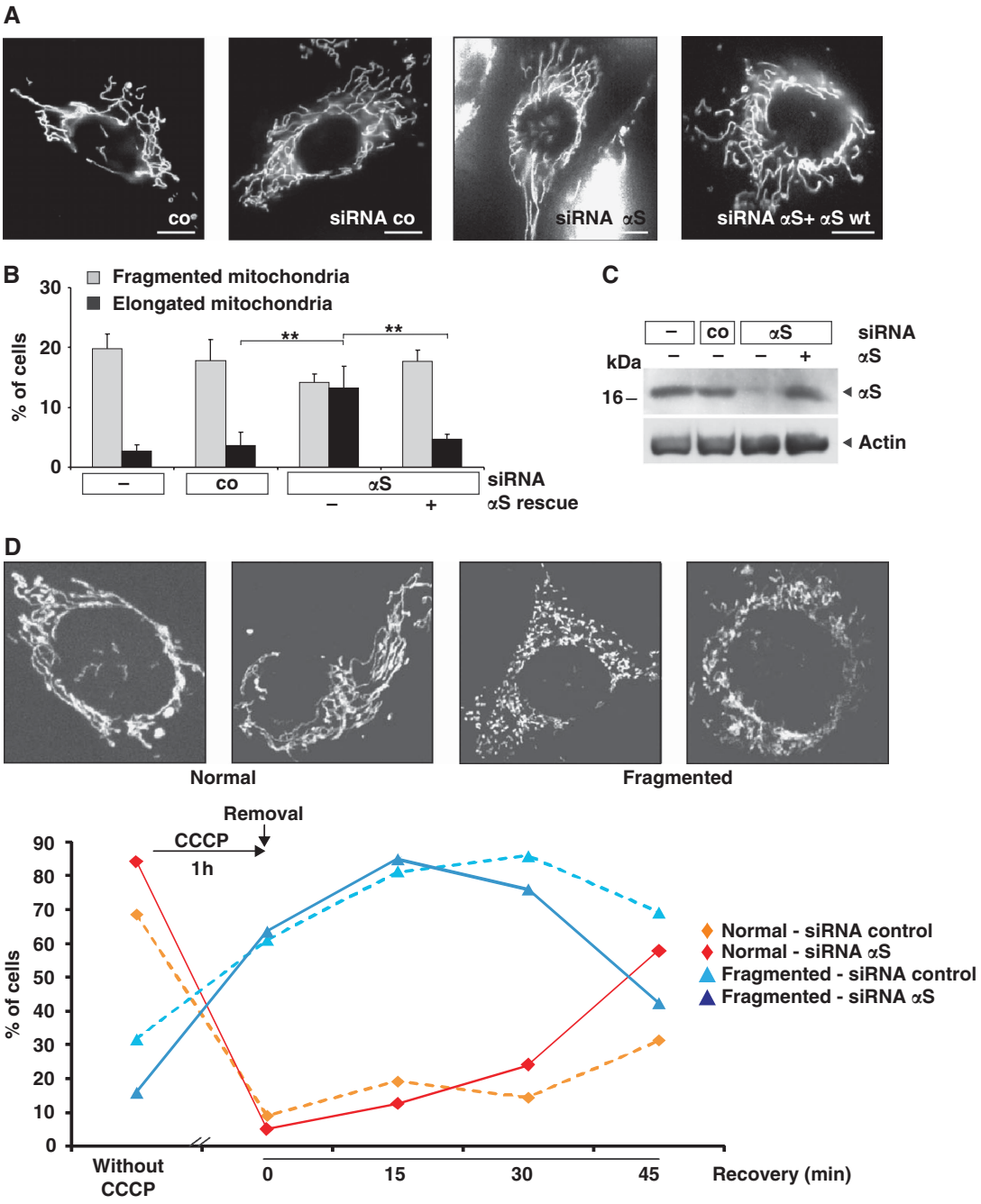

Figure 8 Loss of αS induces elongation of mitochondria. (**A**) Images of fluorescently labelled mitochondria. The panels display representative individual cells either untransfected (co) or transfected with control-siRNA, αS-siRNA, and αS-siRNA + αS-cDNA. Scale bar = 10 μm. (**B**) Statistical analyses of mitochondrial morphology of cells from the experiments shown in (**A**). Approximately 300 cells of each experiment were counted, and the relative amount of cells with changed mitochondrial morphology (i.e. fragmentation or elongation) was determined. Error bars indicate s.d. (**C**) Downregulation of αS in SH-SY5Y cells and retransfection with wild-type αS was monitored by western blotting using β-actin as a loading control. (**D**) Analyses of mitochondrial morphology of cells transfected with a control siRNA or an siRNA against αS before exposure to 10 μM CCCP for 1 h and at different recovery times after removal of CCCP. Insets show images of fluorescently labelled mitochondria. The panels display representative mitochondrial phenotypes as observed before (normal) and after (fragmented) exposure to CCCP. Scale bars = 10 μm. Approximately 60 cells of each experiment were counted, and the relative amount of transfected cells with normal or fragmented mitochondrial morphology was determined. $^{**}P \leqslant 0.01$.

overexpression of αS affects vesicle fusion at the Golgi and not vesicle budding at the ER (Gitler *et al*, 2008). According to our data, these observations may now be attributed to the lipid membrane-binding properties of αS rather than a genetic interaction of αS and the Rab GTPase Ypt1. However, in a cellular context, some organelles might be preferentially bound by αS and binding might depend on αS expression levels. Indeed, in our cell system, a preferential binding to mitochondria was observed. In contrast, in embryonic hippocampal neurons a mild overexpression of αS reduced reclustering of synaptic vesicles, with no apparent change in the rate of fusion (Nemani *et al*, 2010). However, it was unclear if binding of αS to synaptic vesicles was directly affected. Interestingly, our study revealed that the inhibition

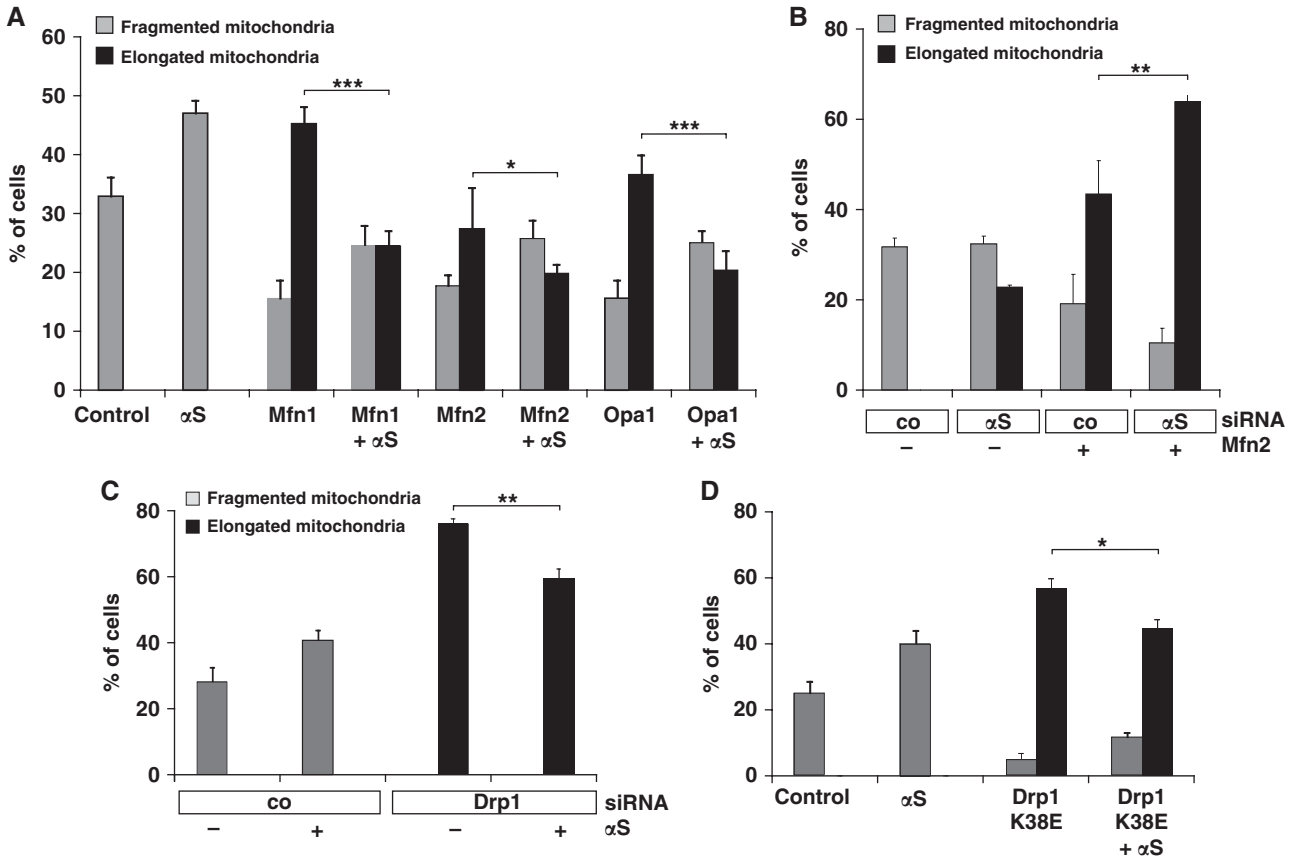

Figure 9 αS-mediated mitochondrial fragmentation is independent of the fusion and fission machinery. (**A**) Cells were transfected with Mfn1, Mfn2, Opa1 and αS as indicated. The relative amounts of cells with changed mitochondrial morphology (i.e. fragmentation or elongation) were determined. (**B**) Cells were transfected with control siRNA or siRNA directed against αS and cotransfected with Mfn2 where indicated. The relative amounts of cells with altered mitochondrial morphology (i.e. fragmentation or elongation) were determined. (**C**) Cells were transfected with control siRNA or Drp1-specific siRNA and cotransfected with αS where indicated, fluorescently labelled and the relative amounts of cells with fragmented or elongated mitochondria were determined. (**D**) Cells were transfected with vector (control), αS and Drp1 K38E where indicated, and the relative amounts of cells with fragmented or elongated mitochondria were determined. Error bars indicate s.d. Expression controls are provided in Supplementary Figure S6. $^{*}P \leqslant 0.05$, $^{**}P \leqslant 0.01$, $^{***}P \leqslant 0.001$.

of mitochondrial fusion by αS could be rescued by coexpression of PINK1, Parkin or DJ-1 but not by the PD related PINK1 G309D and parkin Δ(–79), or by DJ-1 C106A. As PINK1, parkin and DJ-1 have no homologues in *S. cerevisiae*, they could not be found in the extended genome-wide screen (Cooper *et al*, 2006; Gitler *et al*, 2009). Our findings are in line with data from *D. melanogaster*, where αS-induced loss of climbing activity and degeneration of the retina was rescued by PINK1 or parkin (Haywood and Staveley, 2006; Todd and Staveley, 2008). So far, it can only be speculated how this beneficial effect of PINK1 and parkin could be mediated. Obviously, PINK1, parkin and DJ-1 can functionally interact to maintain mitochondrial morphology and function and to protect against adverse effects of αS overexpression. This functional interaction does not necessarily involve a direct interaction between these proteins, it is rather conceivable that different pathways converge at the level of mitochondrial integrity. As PINK1, parkin and DJ-1 are known to protect cells against mitochondrial stress (Canet-Aviles *et al*, 2004; Palacino *et al*, 2004; Kim *et al*, 2005; Clark *et al*, 2006; Park *et al*, 2006; Exner *et al*, 2007; Henn *et al*, 2007; Wood-Kaczmar *et al*, 2008) they could exert a protective effect on mitochondria that counteracts negative effects of αS accumulation. Our data do not exclude that the rescuing effects of the recessive PD-associated genes may work via interaction with the fusion/fission machinery.

Taken together, our findings suggest that αS gene duplications or triplications may lead to increased amounts of αS binding to mitochondria, which inhibits mitochondrial fusion and would therefore trigger disease pathology. In contrast, the missense mutations may rather affect other cellular pathways such as aggregation (Karpinar *et al*, 2009; Tsika *et al*, 2010). Further support to our finding that altered mitochondrial dynamics induced by αS might contribute to PD pathology comes from a recent finding that Pink1 and Parkin affect mitophagy in an ubiquitination-dependent manner (Geisler *et al*, 2010). Therefore, the changes in mitochondrial dynamics and turnover might render neurons susceptible to degeneration in PD.

Materials and methods

Chemicals

Phospholipids (1-palmityl-2-oleoyl-*sn*-glycero-3-phospho-choline (POPC), dipalmitoyl-*sn*-glycero-3-phospho-choline (DPPC), dioleoyl-*sn*-glycero-3-phosphocholine (DOPC), 1-palmityl-2-oleoyl-*sn*-glycero-3-phosphoserine (POPS), dioleoyl-*sn*-glycero-3-phospho-ethanolamine (DOPE) and 1-palmityl-2-oleoyl-*sn*-glycero-3-ethyl-phosphocholine (PC^{+})) were purchased from Avanti Polar Lipids (Alabaster, AL).

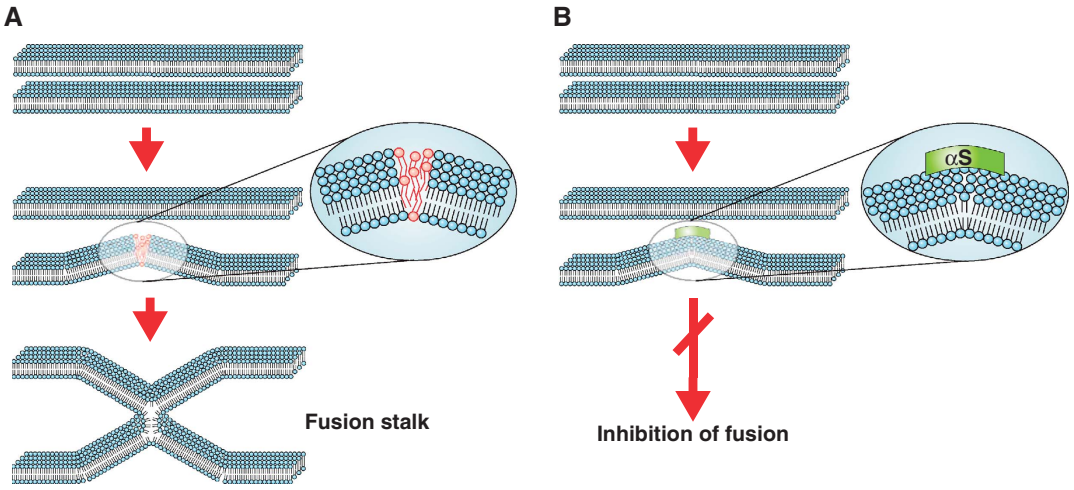

Figure 10 A model of inhibition of membrane fusion by αS. (**A**) Formation of a fusion stalk in the absence of αS. Two membranes achieve close proximity, possibly assisted by a docking machine (not drawn). Curvature in at least one of the fusing membranes causes stress in the packing of the lipids (see inset, the red lipids are not ideally packed), which is necessary to enable fusion of the leaflets of the two fusing membranes and the formation of a fusion stalk. (**B**) Binding of αS to curved membranes seals the packing defects and therefore inhibits the formation of a fusion stalk.

N-(7-nitrobenz-2-oxa-1,3-diazol-4-yl)-1,2-dihexadecanoyl-*sn*-glycero-3-phospho-ethanolamine (NBD-PE) and rhodamine-B 1,2-dihexadecanoyl-*sn*-glycero-3-phosphoethanolamine (Rh-PE) were purchased from Invitrogen. Bovine Brain Sphingomyelin (BBSM), cholesterol, Cytochrome c (MW 13 kDa), Poly-L-lysine (MW 67 kDa), lysozyme (MW 14.3 kDa) and ApoA-I (MW 28.3 kDa) were purchased from Sigma. PEG octa-*n*-dodecylether detergent ($C_{12}E_8$) was purchased from Fluka.

Protein preparations

Recombinant αS (wt-αS) was prepared, purified and desalted as described before (Kahle *et al*, 2001). Lyophilized aliquots were kept at −20°C. Stock solutions of 0.1–0.2 mg/ml αS were kept at 4°C for not longer than 1 week. CD and DLS showed that the protein was in random-coil conformation and that no aggregates were present. The construct αS1–116, lacking the last 24 amino acids from the C-terminus was generated by PCR amplification of the αS gene with the 5′-oligonucleotide primer GGAATTCCATATGGATGTATTCATGA AAGGACTT, and the 3′-oligonucleotide primer GGAATTCCATATG TTACATATCTTCCAGAATTCCTTCCTG containing the *Nde*I restriction site. Amplimers were subcloned into the *Nde*I site of pET-5a (Novagen, San Diego, CA), and constructs used to transform *Escherichia coli* BL21 (DE3). The construct was confirmed by DNA sequencing and the expressed mutant checked by mass spectrometry. Peptides αS (41–65) and αS (116–140) were purchased from PANATecs GmbH.

A cytochrome c stock solution (1 mM) in water was prepared and calibrated with a spectrophotometer using $\varepsilon_{550-539} = 20.1\ mM^{-1}$ for reduced cytochrome c.

Vesicle preparation

SUVs were prepared by sonicating the hydrated lipids 20 min (pulsed mode 20%) under Argon at >5°C above the phase transition temperature of the lipids. SUV were usually diluted to a final lipid concentration of <1 mM to slow down spontaneous fusion. For SUV containing a mixture of lipids, the lipids were first mixed in chloroform. Chloroform was evaporated with nitrogen gas and 1 h vacuum. For cholesterol-containing vesicles, the lipids were mixed in 1 ml of *tert*-butanol. After overnight lyophilization, buffer was added to the lipids. Lipids were always vortexed and hydrated at least 1 h prior to sonication.

Fusion experiments using static light scattering

DPPC-SUV in phosphate buffer (20 mM Na-Phosphate, 100 mM KCl, pH 7.4) were prepared as described above and diluted in a temperature controlled, stirred fluorescence cuvet (2.5 ml) to a final lipid concentration of 600 μM. Static light scattering was measured with a Jasco FP-6300 Fluorimeter with excitation and emission both at 500 nm. Aliquots of protein were added using a Hamilton Syringe through a pinhole in the lid of the instrument. Fusion was initiated by mixing quickly 15 μl of a 5 mM $C_{12}E_8$ stock solution (final $C_{12}E_8$: 30 μM, lipid/detergent ratio = 20 mole/mole).

Lipid-mixing assay

We incorporated 2 mole % NBD-PE and 2 mole % Rhodamine-PE in the vesicles of DPPC-SUV. In these 'donor' vesicles, the fluorescence of NBD was completely quenched by Rhodamine. However, when these vesicles fuse with a 10-fold excess of vesicles without fluorescent probes, lipid-mixing results in dilution of the probes, which neutralizes the quenching effect, that is the NBD-fluorescence increases (Struck *et al*, 1981). Excitation was at 450 nm and emission at 530 nm. Experiments were done at a total lipid concentration of 625 μM, and fusion was triggered with $C_{12}E_8$ (lipid/detergent ratio = 20 mole/mole).

Contents-mixing assay

Vesicles A: 8 mg DPPC hydrated in 1 ml DPA buffer (100 mM KCl, 20 mM Hepes-NaOH, 75 mM DPA, pH 7.4) were sonicated at 45°C for 20 min under Argon. External buffer was replaced by Hepes buffer (20 mM Hepes-NaOH, 150 mM KCl, pH 7.4) using a Sephadex G75 Column, at 45°C, eluting with Hepes buffer. Final lipid concentration was about 5 mM. Vesicles were stored at 45°C to prevent fusion. Vesicles B were prepared as vesicles A, except that Terbium buffer was trapped (100 mM KCl, 20 mM Hepes-NaOH, 75 mM Citrate, 7.5 mM $TbCl_3$, pH 7.4). Fusion experiment: stirred cuvet at 30°C with 1.75 ml Hepes buffer + 2 μl 1 M EDTA (final EDTA concentration 1 mM) + 125 μl Vesicles A + 125 μl vesicles B (final total lipid concentration about 625 μM). Fusion was induced by adding 12.5 μl $C_{12}E_8$ stock solution (final lipid/$C_{12}E_8$ = 20 mole/mole). Formation of the Tb^{3+}–DPA complex due to mixing of the contents of the SUV was revealed by the Terbium fluorescence (λ_{em} = 454 nm, excitation at 276 nm). Any Tb^{3+} that had leaked to the external buffer was bound to EDTA resulting in total suspension of the Terbium fluorescence. The experiment was repeated in the presence of αS (lipid/αS = 200 mole/mole).

Calcium-induced fusion

Fusion assay: donor vesicles (POPS-SUV with 2 mole % NBD-PE and 2 mole % Rhodamine PE) were mixed with a 10-fold excess of acceptor vesicles (POPS-SUV) in 2.5 ml stirred Hepes buffer (20 mM Hepes-NaOH, 100 mM KCl, pH 7.4.) at RT (final donor lipid concentration: 2 μM, acceptor lipid concentration: 20 μM). Fusion was initiated after 2 min by adding 25 μl of a 100 mM $CaCl_2$ stock solution (final $CaCl_2$: 1 mM).

Spontaneous fusion of vesicles with opposite charges measured with stop-flow fluorescence

Experiments were carried out with a Jasco J-810 CD Spectrometer equipped with a BioLogic μSFM-20 stop-flow extension. Fluorescence was measured by setting the photomultiplier at 90 degree angle and placing a 500 nm cutoff filter in front of it. Excitation was at 450 nm with open slit (20 nm). Donor vesicles (SUV of PC^+ with 2% NBD-PE and 2% Rh-PE) were put into one syringe and acceptor vesicles (POPS-SUV) in the other. Equal volumes of both syringes were rapidly mixed and subsequent fluorescence changes monitored after the dead time of mixing (about 8 μs). Final lipid concentration of POPS-SUV was 50 μM and PC^+-SUV was 10 μM.

PEG-induced vesicle fusion

SUV composed of DOPC:DOPE:BBSM:cholesterol (molar ratio 35:30:15:20) were prepared in phosphate buffer (20 mM Na-Phosphate, 100 mM KCl, pH 7.4) by sonication. Fusion of 'donor' vesicles (including 2 mole % NBD-PE and 2 mole % Rh-PE) with a 10-fold excess of 'acceptor' vesicles (containing no fluorescent lipids) was initiated by addition of 4% (w/w) of PEG (Polyethyleneglycol 8000).

Cell culture and transfection

SH-SY5Y human neuroblastoma cells were cultured in DMEM F-12 with glutamine (Lonza) supplemented with 15% (v/v) fetal calf serum, non-essential amino acids (Invitrogen) and penicillin/streptomycin. Transfection was performed with Lipofectamine/Plus (Invitrogen) according to the manufacturer's instructions. Vectors for expression of αS wt, A30P and A53T mutants as described (Hasegawa *et al*, 2004) and for expression of DJ-1 C106A as described (Waak *et al*, 2009) were kindly provided by P Kahle (Laboratory of Functional Neurogenetics, Hertie Institute for Clinical Brain Research, Tübingen, Germany). The following DNA constructs have been described before: PINK1 wt and PINK1 G309D (Exner *et al*, 2007), parkin wt and parkin Δ1–79 (Winklhofer *et al*, 2003; Henn *et al*, 2005), DJ-1 wt (Gorner *et al*, 2004), Mfn2, Opa1, Drp1(K38E)-ECFP (Harder *et al*, 2004; Neuspiel *et al*, 2005), mito-DsRED (Okita *et al*, 2004). The human Mfn1 cDNA sequence (BC040557) was obtained from Open Biosystems and subcloned into pcDNA6A/V5-His (Invitrogen) using *Nhe*I and *Xho*I. βS was subcloned into pcDNA6A/V5 using *Hin*dIII and *Xho*I. Mito-GFP was purchased from Invitrogen. For RNA interference, cells were transfected with HP-validated siRNA directed against the 3′UTR of αS or non-targeting control siRNA (Qiagen). Downregulation of Drp1 was performed as described (Lutz *et al*, 2009).

Fluorescent staining of mitochondria

For visualization of mitochondria, SH-SY5Y cells were cotransfected with mito-GFP (Invitrogen), fixed for 15 min in 4% paraformaldehyde in phosphate-buffered saline (PBS) at room temperature. Coverslips were mounted onto glass slides using ProLong Gold Antifade Reagent (Invitrogen) for analysis. A series of images along the *z* axis were taken with an inverted laser scanning confocal microscope (Zeiss Axiovert 200 M), with a ×100/1.4 DIC oil immersion lens and projected into a single image using the maximal projection tool of the LSM 510 confocal software (Zeiss). For life-cell imaging, SH-SY5Y cells were seeded on poly-L-lysine-coated coverslips. On the day after transfection, cells were fluorescently labelled with 0.1 μM DiOC6(3) (Molecular Probes) in medium for 15 min. Coverslips were rinsed in PBS and living cells were analysed for mitochondrial morphology by fluorescence microscopy using a Leica DMRB microscope. Transfected cells were identified by coexpression of mCherry for life-cell imaging or by coexpression of mito-GFP. Cells that displayed a network of filamentous mitochondria (see Figures 2A and D and 8A; control transfected) were classified as normal, cells with a disrupted network of mitochondria (see Figure 2A; αS wt, A30P and A53T and Figure 2D αS and βS) were classified as fragmented, cells with much extended mitochondrial tubules were classified as elongated (see Figure 8A; siRNA αS). Data are mean values of at least three independent experiments. Fragmentation was induced by incubation of cells in 10 μM carbonyl cyanide 3-chlorophenylhydrazone (CCCP) for 1 h. The medium was replaced by fresh medium without CCCP and after different time points cells were fixed and mounted onto glass slides. Cells that displayed a network of filamentous mitochondria were classified as normal, cells with fragmented or partially re-elongated mitochondria were classified as fragmented.

Measurement of mitochondrial membrane potential with TMRM

SH-SY5Y cells were seeded on poly-L-lysine-coated coverslips. On the day after transfection, cells were fluorescently labelled with 20 nM TMRM (Molecular Probes) in imaging buffer (116 mM NaCl, 5.4 mM KCl, 0.4 mM $MgSO_4$, 20 mM HEPES, 0.9 mM Na_2HPO_4, 1.2 mM $CaCl_2$, 10 mM glucose, 20 mM taurine, 5 mM pyruvate, pH 7.4) for 60 min at room temperature as described (Davidson *et al*, 2007). Pictures were taken with an inverted laser scanning confocal microscope (Zeiss LSM 510 Meta) with a ×100/1.4 DIC oil immersion lens at lowest setting of the HeNe (543 nm) laser. The intensity of the TMRM signal in the area of mito-GFP and TMRM signal colocalization was measured in life cells using the LSM 510 confocal software (Zeiss).

Measurement of cellular ATP levels

Cellular steady-state ATP levels were measured using the ATP Bioluminescence assay kit HS II (Roche Applied Science) according to the manufacturer's instructions. SH-SY5Y cells were plated on six-well plates. After 24 h, cells were transfected using Lipofectamine/Plus (Invitrogen) with the indicated DNA constructs. At 20 h before harvesting cells, the culture medium was replaced by medium containing 3 mM glucose. Cells were washed twice with PBS, scraped off the plate, and lysed according to the provided protocol. Bioluminescence of the samples was determined using an LB96V luminometer (Berthold Technologies), analysed with WinGlow Software (Berthold Technologies) and normalized to total protein levels. Each transfection was performed in duplicate, and all experiments were repeated at least five times.

PEG cellular fusion assay

SH-SY5Y cells were transiently transfected with either mitochondrially targeted green fluorescent protein (mito-GFP) or mitochondrially targeted DsRED (mito-RFP) and either empty vector or αS. At 8 h after transfection, cells were coplated (ratio 1:1) on coverslips and cocultivated for 16 h. Then, fusion of cocultured cells was induced by a 90-s treatment with a pre-warmed solution of 50% (w/v) PEG 3350 in PBS, followed by extensive washing with pre-warmed PBS. After additional cocultivation for 5 h in cell culture medium, cells were fixed with 3.7% (v/v) formaldehyde in PBS. After two washes with PBS, coverslips were mounted and then analysed using confocal microscopy (Zeiss LSM 510 Meta) in a blinded manner. To inhibit *de novo* synthesis of fluorescent proteins, 30 min before PEG treatment cells were incubated with the protein synthesis inhibitor cyclohexymide (40 μg/ml), which was subsequently added to all solutions and tissue culture media until the cells were fixed. Cell hybrids from two independent experiments were analysed in a blinded manner for mitochondrial fusion using Zeiss LSM 510 Meta Software. Per experiment at least 40 cell hybrids were analysed. The percent mitochondrial fusion indicates the rate of overlap between green and red mitochondrially targeted fluorescent proteins expressed in one cell hybrid.

Antibodies

Protein expression was controlled by separation of 0.25% Triton X-100 cell lysates on SDS gels, followed by immunoblotting with the following antibodies: αS rat monoclonal antibody against human αS (116–131) peptide MPVDPDNEAYEMPSEE, (Kahle *et al*, 2000), PINK1 polyclonal antibody BC100–494 (Novus Biologicals), parkin polyclonal antibody 2132 (Cell Signaling), DJ-1 rabbit polyclonal antiserum 3407 (Gorner *et al*, 2007), Mfn1 polyclonal antibody (Novus Biologicals), Mfn2 polyclonal antibody (Sigma), Opa1 polyclonal antibody (Duvezin-Caubet *et al*, 2006) Drp1 monoclonal antibody (BD Transduction Laboratories), Tim23 monoclonal antibody (BD Bioscience), calreticulin polyclonal antibody (Calbiochem), V5 monoclonal antibody (Invitrogen), calnexin polyclonal antibody (StressGen), GFP mouse monoclonal (Roche) and β-actin monoclonal antibody (Sigma). Bound antibodies were detected with the enhanced chemiluminescence detection system (Amersham) or the Immobilon western chemoluminescent HRP substrate (Millipore).

Statistical analysis

Statistical analysis was carried out using ANOVA ($^*P \leqslant 0.05$; $^{**}P \leqslant 0.01$; $^{***}P \leqslant 0.001$).

C. elegans: generation of transgenic animals, fluorescence microscopy

C. elegans strains were cultured at 20°C as described previously (Karpinar *et al*, 2009). To express human αS in *C. elegans* BWMs, αS was fused to mYFP citrine at the C-terminus and cloned under the control of the *myo-3*-promoter in the expression vector pPD115.62 (*Pmyo-3*::*gfp*, kindly provided by A Fire) replacing *gfp* (Karpinar *et al*, 2009). C-terminal fusion of αS with YFP has been used before and it has been shown that it does not significantly change the structure of the protein or its aggregation properties (van Ham *et al*, 2010). To create transgenic *C. elegans* expressing the mitochondrial marker TOM70-CFP in muscle cells, an injection mix containing *Pmyo-3*::*tom70-cfp* (5 ng/μl, kindly provided by A van der Bliek, UCLA) and the coinjection-marker pRF4 (*rol-6(su1006sd)*; 40 ng/μl) was injected into the gonads of young adults as described (Mello *et al*, 1991). To create transgenic worms expressing αS-YFP in addition to the mitochondrial marker, worms were injected with a plasmid mix additionally containing *Pmyo-3*::*αS-yfp* (55 ng/μl for gzEx119 and 30 ng/μl for gzEx120 and gzEx121). All injection mixes were adjusted to a total DNA concentration of 100 ng/μl by addition of pBluescript II (Stratagene). Transgenic animals were imaged on the first day of adulthood while being anaesthetized with 50 mM NaN_3 in M9 buffer and mounted on 2% agarose pads. Imaging was performed using an UltraviewVox spinning disk microscope (Perkin Elmer) with a ×100/1.40 oil immersion objective. The morphological appearance of mitochondria in BWMs of transgenic strains were classified into three categories: (i) wild-type like, (ii) fragmented or (iii) thin and highly interconnected. The classification was done on *z*-stacks, which were projected into a single plane using the extended focus tool of the Volocity software (Perkin Elmer).

In order to analyse the changes in mitochondrial morphology occurring during aging, we compared the mitochondrial morphology in muscle cells of young adult worms (3 days after hatching) with that of worms in the post-reproductive stage (7 days after hatching).

For neuronal expression, the *myo3*-promoter in was replaced by the neuronal *rab-3*-promoter creating *Prab-3*::*tom70-cfp* (5 ng/μl) and *Prab-3*::*αS-yfp* (30 ng/μl), respectively (the respective plasmid concentrations in the injection mixes are indicated). Motor neurons were imaged as described previously for BWMs. Mitochondrial appearance in neuronal cell bodies was classified into three categories: as (i) ring-like, (ii) tubular or (iii) highly fragmented. αS expression levels were determined by western blotting using either a polyclonal rabbit αS antibody (Anaspec) or monoclonal rat αS antibody 15G7 and normalized against α-tubulin using the monoclonal mouse antibody 12G10 (DSHB).

Electron microscopy

Culture cells were grown on Thermonox discs and mounted between two 10 μm deep aluminium platelets (Microscopy Services, Flintbek) and immediately frozen using a BalTec HPM 10. Freeze substitution was carried out in a Leica AFS2. For morphological investigations, incubations were at −90°C for 100 h in 0.1% tannic acid, 7 h in 2% OsO_4, and at −20°C for 16 h in 2% OsO_4, followed by embedding in EPON at RT. For immunostaining, incubations were at −90°C for 100 h in 1.5% uranyl acetate, followed by embedding in Lowicryl HM20 at −45°C (Rostaing *et al*, 2004) (all solutions w/v in dry acetone). EPON sections were 50 nm, Lowicryl sections 90 nm. Lowicryl sections were stained with anti-synuclein antibodies (rabbit, AnaSpec Inc.) and 10 nm Goat-anti-rabbit-gold. Washing was done on 50 mM PBS with 0.05% Tween20. In all, 50 nm EPON sections were post-stained with saturated uranyl acetate in 75% methanol and 4% lead citrate (Reynolds, 1963). In all, 90 nm Lowicryl sections were post-stained with 6% phoshotungstic acid. Micrographs were taken with a 1024 × 1024 CCD detector (Proscan CCD HSS 512/1024; Proscan Electronic Systems, Scheuring, Germany) in a Zeiss EM 902A, operated in the bright field mode.

Supplementary data

Supplementary data are available at *The EMBO Journal* Online (http://www.embojournal.org).

Acknowledgements

This work was supported by the Collaborative Research Center SFB 596 (Projects A14, B10, B13 and B9), the Lüneburg Foundation, the Leibniz Award of the Deutsche Forschungs Gemeinschaft, the German Ministry for Education and Research (NGFN plus 'Functional Genomics of Parkinson's Disease'), the Helmholtz Alliance 'Mental Health in an Ageing Society' and the Center for Integrated Protein Science Munich (CIPSM). C Haass is supported by a 'Forschungsprofessur' of the LMU. N Wender is funded by the Dorothea-Schlözer-Programm of the Georg-August-Universität Göttingen. We thank Sabine Odoy for excellent technical assistance, P Kahle and H McBride for providing plasmids, the Hans and Ilse Breuer Foundation for the confocal microscope and M Klingenberg and H Steiner for critical discussions of the manuscript.

Conflict of interest

The authors declare that they have no conflict of interest.

References

Abeliovich A, Schmitz Y, Farinas I, Choi-Lundberg D, Ho WH, Castillo PE, Shinsky N, Verdugo JM, Armanini M, Ryan A, Hynes M, Phillips H, Sulzer D, Rosenthal A (2000) Mice lacking alpha-synuclein display functional deficits in the nigrostriatal dopamine system. *Neuron* **25:** 239–252

Ben Gedalya T, Loeb V, Israeli E, Altschuler Y, Selkoe DJ, Sharon R (2009) Alpha-synuclein and polyunsaturated fatty acids promote clathrin-mediated endocytosis and synaptic vesicle recycling. *Traffic* **10:** 218–234

Beyer K (2007) Mechanistic aspects of Parkinson's disease. α-synuclein and the biomembrane. *Cell Biochem Biophys* **47:** 285–299

Bodner CR, Dobson CM, Bax A (2009) Multiple tight phospholipid-binding modes of alpha-synuclein revealed by solution NMR spectroscopy. *J Mol Biol* **390:** 775–790

Cabin DE, Shimazu K, Murphy D, Cole NB, Gottschalk W, McIlwain KL, Orrison B, Chen A, Ellis CE, Paylor R, Lu B, Nussbaum RL (2002) Synaptic vesicle depletion correlates with attenuated synaptic responses to prolonged repetitive stimulation in mice lacking alpha-synuclein. *J Neurosci* **22:** 8797–8807

Canet-Aviles RM, Wilson MA, Miller DW, Ahmad R, McLendon C, Bandyopadhyay S, Baptista MJ, Ringe D, Petsko GA, Cookson MR (2004) The Parkinson's disease protein DJ-1 is neuroprotective due to cysteine-sulfinic acid-driven mitochondrial localization. *Proc Natl Acad Sci USA* **101:** 9103–9108

Chandra S, Fornai F, Kwon HB, Yazdani U, Atasoy D, Liu X, Hammer RE, Battaglia G, German DC, Castillo PE, Sudhof TC (2004) Double-knockout mice for alpha- and beta-synucleins: effect on synaptic functions. *Proc Natl Acad Sci USA* **101:** 14966–14971

Chandra S, Gallardo G, Fernandez-Chacon R, Schluter OM, Sudhof TC (2005) Alpha-synuclein cooperates with CSPalpha in preventing neurodegeneration. *Cell* **123:** 383–396

Chen M, Margittai M, Chen J, Langen R (2007) Investigation of alpha-synuclein fibril structure by site-directed spin labeling. *J Biol Chem* **282:** 24970–24979

Chen X, Arac D, Wang TM, Gilpin CJ, Zimmerberg J, Rizo J (2006) SNARE-mediated lipid mixing depends on the physical state of the vesicles. *Biophys J* **90:** 2062–2074

Chernomordik L, Kozlov MM, Zimmerberg J (1995) Lipids in biological membrane fusion. *J Membr Biol* **146:** 1–14

Chernomordik LV, Kozlov MM (2003) Protein-lipid interplay in fusion and fission of biological membranes. *Annu Rev Biochem* **72:** 175–207

Chiba-Falek O, Lopez GJ, Nussbaum RL (2006) Levels of alpha-synuclein mRNA in sporadic Parkinson disease patients. *Mov Disord* **21:** 1703–1708

Cho DH, Nakamura T, Lipton SA (2010) Mitochondrial dynamics in cell death and neurodegeneration. *Cell Mol Life Sci* (in press)

Clark IE, Dodson MW, Jiang C, Cao JH, Huh JR, Seol JH, Yoo SJ, Hay BA, Guo M (2006) Drosophila pink1 is required for mitochondrial

function and interacts genetically with parkin. *Nature* **441:** 1162–1166

Cole NB, Dieuliis D, Leo P, Mitchell DC, Nussbaum RL (2008) Mitochondrial translocation of alpha-synuclein is promoted by intracellular acidification. *Exp Cell Res* **314:** 2076–2089

Cooper AA, Gitler AD, Cashikar A, Haynes CM, Hill KJ, Bhullar B, Liu K, Xu K, Strathearn KE, Liu F, Cao S, Caldwell KA, Caldwell GA, Marsischky G, Kolodner RD, Labaer J, Rochet JC, Bonini NM, Lindquist S (2006) Alpha-synuclein blocks ER-Golgi traffic and Rab1 rescues neuron loss in Parkinson's models. *Science* **313:** 324–328

Cornell RB, Taneva SG (2006) Amphipathic helices as mediators of the membrane interaction of amphitropic proteins, and as modulators of bilayer physical properties. *Curr Protein Pept Sci* **7:** 539–552

Dagda RK, Cherra III SJ, Kulich SM, Tandon A, Park D, Chu CT (2009) Loss of PINK1 function promotes mitophagy through effects on oxidative stress and mitochondrial fission. *J Biol Chem* **284:** 13843–13855

Davidson SM, Yellon D, Duchen MR (2007) Assessing mitochondrial potential, calcium, and redox state in isolated mammalian cells using confocal microscopy. *Methods Mol Biol* **372:** 421–430

Davidson WS, Jonas A, Clayton DF, George JM (1998) Stabilization of α-synuclein secondary structue upon bindung to synthetic membranes. *J Biol Chem* **273:** 9443–9449

Dennison SM, Bowen ME, Brunger AT, Lentz BR (2006) Neuronal SNAREs do not trigger fusion between synthetic membranes but do promote PEG-mediated membrane fusion. *Biophys J* **90:** 1661–1675

Der-Sarkissian A, Jao CC, Chen J, Langen R (2003) Structural organization of α-synuclein fibrils studied by site-directed spin labeling. *J Biol Chem* **278:** 37530–37535

Derksen A, Gantz D, Small DM (1996) Calorimetry of apolipoprotein-A1 binding to phosphatidylcholine-triolein-cholesterol emulsions. *Biophys J* **70:** 330–338

Detmer SA, Chan DC (2007) Functions and dysfunctions of mitochondrial dynamics. *Nat Rev Mol Cell Biol* **8:** 870–879

Devi L, Raghavendran V, Prabhu BM, Avadhani NG, Anandatheerthavarada HK (2008) Mitochondrial import and accumulation of {alpha}-sy. *J Biol Chem* **283:** 9089–9100

Dobson CM (2003) Protein folding and misfolding. *Nature* **426:** 884–890

Drescher M, Godschalk F, Veldhuis G, van Rooijen BD, Subramaniam V, Huber M (2008a) Spin-label EPR on alpha-synuclein reveals differences in the membrane binding affinity of the two antiparallel helices. *Chembiochem* **9:** 2411–2416

Drescher M, Veldhuis G, van Rooijen BD, Milikisyants S, Subramaniam V, Huber M (2008b) Antiparallel arrangement of the helices of vesicle-bound alpha-synuclein. *J Am Chem Soc* **130:** 7796–7797

Duvezin-Caubet S, Jagasia R, Wagener J, Hofmann S, Trifunovic A, Hansson A, Chomyn A, Bauer MF, Attardi G, Larsson NG, Neupert W, Reichert AS (2006) Proteolytic processing of OPA1 links mitochondrial dysfunction to alterations in mitochondrial morphology. *J Biol Chem* **281:** 37972–37979

Exner N, Treske B, Paquet D, Holmstrom K, Schiesling C, Gispert S, Carballo-Carbajal I, Berg D, Hoepken HH, Gasser T, Kruger R, Winklhofer KF, Vogel F, Reichert AS, Auburger G, Kahle PJ, Schmid B, Haass C (2007) Loss-of-function of human PINK1 results in mitochondrial pathology and can be rescued by parkin. *J Neurosci* **27:** 12413–12418

Ferreon AC, Gambin Y, Lemke EA, Deniz AA (2009) Interplay of alpha-synuclein binding and conformational switching probed by single-molecule fluorescence. *Proc Natl Acad Sci USA* **106:** 5645–5650

Fujita Y, Ohama E, Takatama M, Al-Sarraj S, Okamoto K (2006) Fragmentation of Golgi apparatus of nigral neurons with alpha-synuclein-positive inclusions in patients with Parkinson's disease. *Acta Neuropathol* **112:** 261–265

Gaber BP, Sheridan JP (1982) Kinetic and thermodynamic studies of the fusion of small unilamellar phospholipid vesicles. *Biochim Biophys Acta* **685:** 87–93

Geisler S, Holmstrom KM, Skujat D, Fiesel FC, Rothfuss OC, Kahle PJ, Springer W (2010) PINK1/Parkin-mediated mitophagy is dependent on VDAC1 and p62/SQSTM1. *Nat Cell Biol* **12:** 119–131

Giannakis E, Pacifico J, Smith DP, Hung LW, Masters CL, Cappai R, Wade JD, Barnham KJ (2008) Dimeric structures of alpha-synuclein bind preferentially to lipid membranes. *Biochim Biophys Acta* **1778:** 1112–1119

Gitler AD, Bevis BJ, Shorter J, Strathearn KE, Hamamichi S, Su LJ, Caldwell KA, Caldwell GA, Rochet JC, McCaffery JM, Barlowe C, Lindquist S (2008) The Parkinson's disease protein alpha-synuclein disrupts cellular Rab homeostasis. *Proc Natl Acad Sci USA* **105:** 145–150

Gitler AD, Chesi A, Geddie ML, Strathearn KE, Hamamichi S, Hill KJ, Caldwell KA, Caldwell GA, Cooper AA, Rochet JC, Lindquist S (2009) Alpha-synuclein is part of a diverse and highly conserved interaction network that includes PARK9 and manganese toxicity. *Nat Genet* **41:** 308–315

Gorner K, Holtorf E, Odoy S, Nuscher B, Yamamoto A, Regula JT, Beyer K, Haass C, Kahle PJ (2004) Differential effects of Parkinson's disease-associated mutations on stability and folding of DJ-1. *J Biol Chem* **279:** 6943–6951

Gorner K, Holtorf E, Waak J, Pham TT, Vogt-Weisenhorn DM, Wurst W, Haass C, Kahle PJ (2007) Structural determinants of the C-terminal helix-kink-helix motif essential for protein stability and survival promoting activity of DJ-1. *J Biol Chem* **282:** 13680–13691

Gosavi N, Lee HJ, Lee JS, Patel S, Lee SJ (2002) Golgi fragmentation occurs in the cells with prefibrillar alpha-synuclein aggregates and precedes the formation of fibrillar inclusion. *J Biol Chem* **277:** 48984–48992

Grundemann J, Schlaudraff F, Haeckel O, Liss B (2008) Elevated alpha-synuclein mRNA levels in individual UV-laser-microdissected dopaminergic substantia nigra neurons in idiopathic Parkinson's disease. *Nucleic Acids Res* **36:** e38

Gursky O (2005) Apolipoprotein structure and dynamics. *Curr Opin Lipidol* **16:** 287–294

Haass C, Selkoe DJ (2007) Soluble protein oligomers in neurodegeneration: lessons from the Alzheimer's amyloid beta-peptide. *Nat Rev Mol Cell Biol* **8:** 101–112

Haque ME, McIntosh TJ, Lentz BR (2001) Influence of lipid composition on physical properties and PEG-mediated fusion of curved and uncurved model membrane vesicles: 'nature's own fusogenic lipid bilayer'. *Biochemistry* **40:** 4340–4348

Harder Z, Zunino R, McBride H (2004) Sumo1 conjugates mitochondrial substrates and participates in mitochondrial fission. *Curr Biol* **14:** 340–345

Hasegawa T, Matsuzaki M, Takeda A, Kikuchi A, Akita H, Perry G, Smith MA, Itoyama Y (2004) Accelerated alpha-synuclein aggregation after differentiation of SH-SY5Y neuroblastoma cells. *Brain Res* **1013:** 51–59

Haywood AF, Staveley BE (2006) Mutant alpha-synuclein-induced degeneration is reduced by parkin in a fly model of Parkinson's disease. *Genome* **49:** 505–510

Henn IH, Bouman L, Schlehe JS, Schlierf A, Schramm JE, Wegener E, Nakaso K, Culmsee C, Berninger B, Krappmann D, Tatzelt J, Winklhofer KF (2007) Parkin mediates neuroprotection through activation of IkappaB kinase/nuclear factor-kappaB signaling. *J Neurosci* **27:** 1868–1878

Henn IH, Gostner JM, Lackner P, Tatzelt J, Winklhofer KF (2005) Pathogenic mutations inactivate parkin by distinct mechanisms. *J Neurochem* **92:** 114–122

Herndon LA, Schmeissner PJ, Dudaronek JM, Brown PA, Listner KM, Sakano Y, Paupard MC, Hall DH, Driscoll M (2002) Stochastic and genetic factors influence tissue-specific decline in ageing C. elegans. *Nature* **419:** 808–814

Hoppert M (2003) *Microscopic Techniques in Biotechnology*. Weinheim: Wiley-VCH

Hsu LJ, Sagara Y, Arroyo A, Rockenstein E, Sisk A, Mallory M, Wong J, Takenouchi T, Hashimoto M, Masliah E (2000) alpha-synuclein promotes mitochondrial deficit and oxidative stress. *Am J Pathol* **157:** 401–410

Ibanez P, Bonnet AM, Debarges B, Lohmann E, Tison F, Pollak P, Agid Y, Durr A, Brice A (2004) Causal relation between alpha-synuclein gene duplication and familial Parkinson's disease. *Lancet* **364:** 1169–1171

Ishihara N, Jofuku A, Eura Y, Mihara K (2003) Regulation of mitochondrial morphology by membrane potential, and DRP1-dependent division and FZO1-dependent fusion reaction in mammalian cells. *Biochem Biophys Res Commun* **301:** 891–898

Iwai A, Masliah E, Yoshimoto M, Ge N, Flanagan L, de Silva HA, Kittel A, Saitoh T (1995) The precursor protein of non-A beta

component of Alzheimer's disease amyloid is a presynaptic protein of the central nervous system. *Neuron* **14:** 467–475

Jao CC, Hegde BG, Chen J, Haworth IS, Langen R (2008) Structure of membrane-bound alpha-synuclein from site-directed spin labeling and computational refinement. *Proc Natl Acad Sci USA* **105:** 19666–19671

Jensen PH, Nielsen MS, Jakes R, Dotti CG, Goedert M (1998) Binding of alpha-synuclein to brain vesicles is abolished by familial Parkinson's disease mutation. *J Biol Chem* **273:** 26292–26294

Jo E, Darabie AA, Han K, Tandon A, Fraser PE, McLaurin J (2004) alpha-Synuclein-synaptosomal membrane interactions: implications for fibrillogenesis. *Eur J Biochem* **271:** 3180–3189

Kahle PJ, Neumann M, Ozmen L, Muller V, Jacobsen H, Schindzielorz A, Okochi M, Leimer U, van Der Putten H, Probst A, Kremmer E, Kretzschmar HA, Haass C (2000) Subcellular localization of wild-type and Parkinson's disease-associated mutant alpha-synuclein in human and transgenic mouse brain. *J Neurosci* **20:** 6365–6373

Kahle PJ, Neumann M, Ozmen L, Müller V, Odoy S, Okamoto N, Jacobsen H, Iwatsubo T, Trojanowski JQ, Takahashi H, Wakabayashi K, Bogdanovic N, Riederer P, Kreschmar HA, Haass C (2001) Selective insolubility of alpha-synuclein in human Lewy Body diseases is recapitulated in a transgenic mouse model. *Am J Pathol* **159:** 2215–2225

Kamp F, Beyer K (2006) Binding of α-synuclein affects the lipid packing in bilayers of small vesicles. *J Biol Chem* **281:** 9251–9259

Karpinar DP, Balija MB, Kugler S, Opazo F, Rezaei-Ghaleh N, Wender N, Kim HY, Taschenberger G, Falkenburger BH, Heise H, Kumar A, Riedel D, Fichtner L, Voigt A, Braus GH, Giller K, Becker S, Herzig A, Baldus M, Jackle H *et al* (2009) Pre-fibrillar alpha-synuclein variants with impaired beta-structure increase neurotoxicity in Parkinson's disease models. *EMBO J* **28:** 3256–3268

Kayed R, Pensalfini A, Margol L, Sokolov Y, Sarsoza F, Head E, Hall J, Glabe C (2009) Annular protofibrils are a structurally and functionally distinct type of amyloid oligomer. *J Biol Chem* **284:** 4230–4237

Kim RH, Smith PD, Aleyasin H, Hayley S, Mount MP, Pownall S, Wakeham A, You-Ten AJ, Kalia SK, Horne P, Westaway D, Lozano AM, Anisman H, Park DS, Mak TW (2005) Hypersensitivity of DJ-1-deficient mice to 1-methyl-4-phenyl-1,2,3,6-tetrahydropyrindine (MPTP) and oxidative stress. *Proc Natl Acad Sci USA* **102:** 5215–5220

Kitada T, Asakawa S, Hattori N, Matsumine H, Yamamura Y, Minoshima S, Yokochi M, Mizuno Y, Shimizu N (1998) Mutations in the parkin gene cause autosomal recessive juvenile parkinsonism. *Nature* **392:** 605–608

Kostka M, Hogen T, Danzer KM, Levin J, Habeck M, Wirth A, Wagner R, Glabe CG, Finger S, Heinzelmann U, Garidel P, Duan W, Ross CA, Kretzschmar H, Giese A (2008) Single-particle characterization of iron-induced pore-forming alpha -synuclein oligomers. *J Biol Chem* **283:** 10992–11003

Kramer ML, Schulz-Schaeffer WJ (2007) Presynaptic alpha-synuclein aggregates, not Lewy bodies, cause neurodegeneration in dementia with Lewy bodies. *J Neurosci* **27:** 1405–1410

Labrousse AM, Zappaterra MD, Rube DA, VanderBliek AM (1999) C. elegans dynamin-related protein DRP-1 controls severing of the mitochondrial outer membrane. *Mol Cell* **4:** 815–826

Larsen KE, Schmitz Y, Troyer MD, Mosharov E, Dietrich P, Quazi AZ, Savalle M, Nemani V, Chaudhry FA, Edwards RH, Stefanis L, Sulzer D (2006) α-Synuclein overexpression in PC12 and chromaffin cells impairs catecholamine release by interfering with a late step in exocytosis. *J Neurosci* **26:** 11915–11922

Lee HJ, Khoshaghideh F, Lee S, Lee SJ (2006) Impairment of microtubule-dependent trafficking by overexpression of alpha-synuclein. *Eur J Neurosci* **24:** 3153–3162

Lee HJ, Khoshaghideh F, Patel S, Lee SJ (2004a) Clearance of alpha-synuclein oligomeric intermediates via the lysosomal degradation pathway. *J Neurosci* **24:** 1888–1896

Lee JC, Langen R, Hummel PA, Gray HB, Winkler JR (2004b) Alpha-synuclein structures from fluorescence energy-transfer kinetics: implications for the role of the protein in Parkinson's disease. *Proc Natl Acad Sci USA* **101:** 16466–16471

Lei G, MacDonald RC (2003) Lipid bilayer vesicle fusion: intermediates captured by high-speed microfluorescence spectroscopy. *Biophys J* **85:** 1585–1599

Lentz BR (2007) PEG as a tool to gain insight into membrane fusion. *Eur Biophys J* **36:** 315–326

Li WW, Yang R, Guo JC, Ren HM, Zha XL, Cheng JS, Cai DF (2007) Localization of alpha-synuclein to mitochondria within midbrain of mice. *Neuroreport* **18:** 1543–1546

Liu T, Tucker WC, Bhalla A, Chapman ER, Weisshaar JC (2005) SNARE-driven, 25-millisecond vesicle fusion *in vitro*. *Biophys J* **89:** 2458–2472

Lutz AK, Exner N, Fett ME, Schlehe JS, Kloos K, Laemmermann K, Brunner B, Kurz-Drexler A, Vogel F, Reichert AS, Bouman L, Vogt-Weisenhorn D, Wurst W, Tatzelt J, Haass C, Winklhofer KF (2009) Loss of parkin or PINK1 function increases DRP1-dependent mitochondrial fragmentation. *J Biol Chem* **284:** 22938–22951

Malka F, Aure K, Goffart S, Spelbrink JN, Rojo M (2007) The mitochondria of cultured mammalian cells: I. Analysis by immunofluorescence microscopy, histochemistry, subcellular fractionation, and cell fusion. *Methods Mol Biol* **372:** 3–16

Maraganore DM, de Andrade M, Elbaz A, Farrer MJ, Ioannidis JP, Kruger R, Rocca WA, Schneider NK, Lesnick TG, Lincoln SJ, Hulihan MM, Aasly JO, Ashizawa T, Chartier-Harlin MC, Checkoway H, Ferrarese C, Hadjigeorgiou G, Hattori N, Kawakami H, Lambert JC *et al* (2006) Collaborative analysis of alpha-synuclein gene promoter variability and Parkinson disease. *JAMA* **296:** 661–670

Maroteaux L, Campanelli JT, Scheller RH (1988) Synuclein: a neuron-specific protein localized to the nucleus and presynaptic nerve terminal. *J Neurosci* **8:** 2804–2815

Martin LJ, Pan Y, Price AC, Sterling W, Copeland NG, Jenkins NA, Price DL, Lee MK (2006) Parkinson's disease alpha-synuclein transgenic mice develop neuronal mitochondrial degeneration and cell death. *J Neurosci* **26:** 41–50

Mello CC, Kramer JM, Stinchcomb D, Ambros V (1991) Efficient gene transfer in C. elegans: extrachromosomal maintenance and integration of transforming sequences. *EMBO J* **10:** 3959–3970

Morais VA, Verstreken P, Roethig A, Smet J, Snellinx A, Vanbrabant M, Haddad D, Frezza C, Mandemakers W, Vogt-Weisenhorn D, Van Coster R, Wurst W, Scorrano L, De Strooper B (2009) Parkinson's disease mutations in PINK1 result in decreased complex I activity and deficient synaptic function. *EMBO Mol Med* **1:** 99–111

Murphy DD, Rueter SM, Trojanowski JQ, Lee VM (2000) Synucleins are developmentally expressed, and alpha-synuclein regulates the size of the presynaptic vesicular pool in primary hippocampal neurons. *J Neurosci* **20:** 3214–3220

Nakamura K, Nemani VM, Wallender EK, Kaehlcke K, Ott M, Edwards RH (2008) Optical reporters for the conformation of alpha-synuclein reveal a specific interaction with mitochondria. *J Neurosci* **28:** 12305–12317

Nemani VM, Lu W, Berge V, Nakamura K, Onoa B, Lee MJ, Chaudhry FA, Nicoli RA, Edwards RH (2010) Increased expression of alpha-synuclein reduces neurotransmitter release by inhibiting synaptic vesicle reclustering after endocytosis. *Neuron* **65:** 66–79

Neuspiel M, Zunino R, Gangaraju S, Rippstein P, McBride H (2005) Activated mitofusin 2 signals mitochondrial fusion, interferes with Bax activation, and reduces susceptibility to radical induced depolarization. *J Biol Chem* **280:** 25060–25070

Nickel W, Weber T, McNew JA, Parlati F, Sollner TH, Rothman JE (1999) Content mixing and membrane integrity during membrane fusion driven by pairing of isolated v-SNAREs and t-SNAREs. *Proc Natl Acad Sci USA* **96:** 12571–12576

Niemann A, Ruegg M, La Padula V, Schenone A, Suter U (2005) Ganglioside-induced differentiation associated protein 1 is a regulator of the mitochondrial network: new implications for Charcot-Marie-Tooth disease. *J Cell Biol* **170:** 1067–1078

Nuscher B, Kamp F, Mehnert T, Odoy S, Haass C, Kahle PJ, Beyer K (2004) α-synuclein has a high affinity for packing defects in a bilayer membrane. A thermodynamics study. *J Biol Chem* **21:** 21966–21975

Okita C, Sato M, Schroeder T (2004) Generation of optimized yellow and red fluorescent proteins with distinct subcellular localization. *Biotechniques* **36:** 418–422, 424

Orth M, Tabrizi SJ, Schapira AH, Cooper JM (2003) Alpha-synuclein expression in HEK293 cells enhances the mitochondrial sensitivity to rotenone. *Neurosci Lett* **351:** 29–32

Palacino JJ, Sagi D, Goldberg MS, Krauss S, Motz C, Wacker M, Klose J, Shen J (2004) Mitochondrial dysfunction and oxidative damage in parkin-deficient mice. *J Biol Chem* **279:** 18614–18622

Pantazatos DP, MacDonald RC (1999) Directly observed membrane fusion between oppositely charged phospholipid bilayers. *J Membr Biol* **170:** 27–38

Parihar MS, Parihar A, Fujita M, Hashimoto M, Ghafourifar P (2008) Mitochondrial association of alpha-synuclein causes oxidative stress. *Cell Mol Life Sci* **65:** 1272–1284

Parihar MS, Parihar A, Fujita M, Hashimoto M, Ghafourifar P (2009) Alpha-synuclein overexpression and aggregation exacerbates impairment of mitochondrial functions by augmenting oxidative stress in human neuroblastoma cells. *Int J Biochem Cell Biol* **41:** 2015–2024

Park J, Lee SB, Lee S, Kim Y, Song S, Kim S, Bae E, Kim J, Shong M, Kim JM, Chung J (2006) Mitochondrial dysfunction in Drosophila PINK1 mutants is complemented by parkin. *Nature* **441:** 1157–1161

Perlmutter JD, Braun AR, Sachs JN (2009) Curvature dynamics of α-synuclein familial Parkinson disease mutants: molecular simulations of the micelle- and bilayer-bound forms. *J Biol Chem* **284:** 7177–7189

Piomelli D, Astarita G, Rapaka R (2007) A neuroscientist's guide to lipidomics. *Nat Rev* **8:** 743–754

Ramakrishnan M, Jensen PH, Marsh D (2006) Association of alpha-synuclein and mutants with lipid membranes: spin-label ESR and polarized IR. *Biochemistry* **45:** 3386–3395

Reynolds ES (1963) The use of lead citrate at high pH as an electron-opaque stain in electron microscopy. *J Cell Biol* **17:** 208–212

Rostaing P, Weimer RM, Jorgensen EM, Triller A, Bessereau JL (2004) Preservation of immunoreactivity and fine structure of adult C. elegans tissues using high-pressure freezing. *J Histochem Cytochem* **52:** 1–12

Sandebring A, Thomas KJ, Beilina A, van der Brug M, Cleland MM, Ahmad R, Miller DW, Zambrano I, Cowburn RF, Behbahani H, Cedazo-Minguez A, Cookson MR (2009) Mitochondrial alterations in PINK1 deficient cells are influenced by calcineurin-dependent dephosphorylation of dynamin-related protein 1. *PLoS One* **4:** e5701

Satake W, Nakabayashi Y, Mizuta I, Hirota Y, Ito C, Kubo M, Kawaguchi T, Tsunoda T, Watanabe M, Takeda A, Tomiyama H, Nakashima K, Hasegawa K, Obata F, Yoshikawa T, Kawakami H, Sakoda S, Yamamoto M, Hattori N, Murata M *et al* (2009) Genome-wide association study identifies common variants at four loci as genetic risk factors for Parkinson's disease. *Nat Genet* **41:** 1303–1307

Schullery SE, Schmidt CF, Felgner P, Tillack TW, Thompson TE (1980a) Fusion of dipalmitoylphosphatidylcholine vesicles. *Biochemistry* **19:** 3919–3923

Schullery SE, Schmidt CF, Felgner P, Tillack TW, Thompson TE (1980b) Fusion of dipalmitoylphosphatidylcholine vesicles. *Biochemistry* **19:** 3919–3923

Sharon R, Bar-Joseph I, Frosch MP, Walsh DM, Hamilton JA, Selkoe DJ (2003) The formation of highly soluble oligomers of α-synuclein is regulated by fatty acids and enhanced in Parkinson's disease. *Neuron* **37:** 583–595

Shavali S, Brown-Borg HM, Ebadi M, Porter J (2008) Mitochondrial localization of alpha-synuclein protein in alpha-synuclein overexpressing cells. *Neurosci Lett* **439:** 125–128

Simon-Sanchez J, Schulte C, Bras JM, Sharma M, Gibbs JR, Berg D, Paisan-Ruiz C, Lichtner P, Scholz SW, Hernandez DG, Kruger R, Federoff M, Klein C, Goate A, Perlmutter J, Bonin M, Nalls MA, Illig T, Gieger C, Houlden H *et al* (2009) Genome-wide association study reveals genetic risk underlying Parkinson's disease. *Nat Genet* **41:** 1308–1312

Singleton AB, Farrer M, Johnson J, Singleton A, Hague S, Kachergus J, Hulihan M, Peuralinna T, Dutra A, Nussbaum R, Lincoln S, Crawley A, Hanson M, Maraganore D, Adler C, Cookson MR, Muenter M, Baptista M, Miller D, Blancato J *et al* (2003) alpha-Synuclein locus triplication causes Parkinson's disease. *Science* **302:** 841

Smith WW, Jiang H, Pei Z, Tanaka Y, Morita H, Sawa A, Dawson VL, Dawson TM, Ross CA (2005) Endoplasmic reticulum stress and mitochondrial cell death pathways mediate A53T mutant alpha-synuclein-induced toxicity. *Hum Mol Genet* **14:** 3801–3811

Spillantini MG, Schmidt ML, Lee VM, Trojanowski JQ, Jakes R, Goedert M (1997) Alpha-synuclein in Lewy bodies. *Nature* **388:** 839–840

Struck DK, Hoekstra D, Pagano RE (1981) Use of resonance energy transfer to monitor membrane fusion. *Biochemistry* **20:** 4093–4099

Takamori S, Holt M, Stenius K, Lemke EA, Gronborg M, Riedel D, Urlaub H, Schenck S, Brugger B, Ringler P, Muller SA, Rammner B, Grater F, Hub JS, De Groot BL, Mieskes G, Moriyama Y, Klingauf J, Grubmuller H, Heuser J *et al* (2006) Molecular anatomy of a trafficking organelle. *Cell* **127:** 831–846

Tamm LK, Crane J, Kiessling V (2003) Membrane fusion: a structural perspective on the interplay of lipids and proteins. *Curr Opin Struct Biol* **13:** 453–466

Todd AM, Staveley BE (2008) Pink1 suppresses alpha-synuclein-induced phenotypes in a Drosophila model of Parkinson's disease. *Genome* **51:** 1040–1046

Trexler A, Rhoades E (2009) α-Synuclein binds large unilamellar vesicles as an extended helix. *Biochemistry* **48:** 2304–2306

Tsika E, Moysidou M, Guo J, Cushman M, Gannon P, Sandaltzopoulos R, Giasson BI, Krainc D, Ischiropoulos H, Mazzulli JR (2010) Distinct region-specific alpha-synuclein oligomers in A53T transgenic mice: implications for neurodegeneration. *J Neurosci* **30:** 3409–3418

Ulmer TS, Bax A (2005) Comparison of structure and dynamics of micelle-bound human alpha-synuclein and Parkinson disease variants. *J Biol Chem* **280:** 43179–43187

Ulmer TS, Bax A, Cole NB, Nussbaum RL (2005) Structure and dynamics of micelle-bound human alpha-synuclein. *J Biol Chem* **280:** 9595–9603

Uversky VN (2002) What does it mean to be natively unfolded? *Eur J Biochem* **269:** 2–12

Uversky VN (2007) Neuropathology, biochemistry, and biophysics of alpha-synuclein aggregation. *J Neurochem* **103:** 17–37

Valente EM, Abou-Sleiman PM, Caputo V, Muqit MM, Harvey K, Gispert S, Ali Z, Del Turco D, Bentivoglio AR, Healy DG, Albanese A, Nussbaum R, Gonzalez-Maldonado R, Deller T, Salvi S, Cortelli P, Gilks WP, Latchman DS, Harvey RJ, Dallapiccola B *et al* (2004) Hereditary early-onset Parkinson's disease caused by mutations in PINK1. *Science* **304:** 1158–1160

van Ham TJ, Esposito A, Kumita JR, Hsu ST, Kaminski Schierle GS, Kaminski CF, Dobson CM, Nollen EA, Bertoncini CW (2010) Towards multiparametric fluorescent imaging of amyloid formation: studies of a YFP model of alpha-synuclein aggregation. *J Mol Biol* **395:** 627–642

Waak J, Weber SS, Gorner K, Schall C, Ichijo H, Stehle T, Kahle PJ (2009) Oxidizable residues mediating protein stability and cytoprotective interaction of DJ-1 with apoptosis signal-regulating kinase 1. *J Biol Chem* **284:** 14245–14257

Weber T, Zemelman BV, McNew JA, Westermann B, Gmachl M, Parlati F, Sollner TH, Rothman JE (1998) SNAREpins: minimal machinery for membrane fusion. *Cell* **92:** 759–772

Weinreb G, Lentz BR (2007) Analysis of membrane fusion as a two-state sequential process: evaluation of the stalk model. *Biophys J* **92:** 4012–4029

Westermann B (2008) Molecular machinery of mitochondrial fusion and fission. *J Biol Chem* **283:** 13501–13505

Wilschut J, Düzgünes N, Fraley R, Papahadjopoulos D (1980) Studies on the mechanism of membrane fusion: kinetics of calcium ion induced fusion of phosphatidylserine vesicles followed by a new assay for mixing of aqueous vesicles contents. *Biochemistry* **1980:** 6011–6021

Winklhofer KF, Henn IH, Kay-Jackson PC, Heller U, Tatzelt J (2003) Inactivation of parkin by oxidative stress and C-terminal truncations: a protective role of molecular chaperones. *J Biol Chem* **278:** 47199–47208

Wood-Kaczmar A, Gandhi S, Yao Z, Abramov AY, Miljan EA, Keen G, Stanyer L, Hargreaves I, Klupsch K, Deas E, Downward J, Mansfield L, Jat P, Taylor J, Heales S, Duchen MR, Latchman D, Tabrizi SJ, Wood NW (2008) PINK1 is necessary for long term survival and mitochondrial function in human dopaminergic neurons. *PLoS One* **3:** e2455

Yavich L, Tanila H, Vepsalainen S, Jakala P (2004) Role of alpha-synuclein in presynaptic dopamine recruitment. *J Neurosci* **24:** 11165–11170

Zhang F, Rowe ES (1994) Calorimetric studies of the interactions of cytochrome c with dioleoylphosphatidylglycerol extruded vesicles: ionic strength effects. *Biochim Biophys Acta* **1193:** 219–225